UNIVERSTIY OF CALIFORNIA, SAN DIEGO

Nanoparticles Patterning by Directed Electric Field Assembly and Photolithography

A dissertation submitted in partial satisfaction of the requirements for the degree

Doctor of Philosophy

in

Electrical Engineering (Nanoscale Devices and Systems)

by

Youngjun Song

Committee in charge:

Professor Michael J. Heller, Chair
Professor Yeshaiahu Fainman, Co-Chair
Professor Shaochen Chen
Professor Sadik Esener
Professor Yu-hwa Lo

2014

The Dissertation of Youngjun Song is approved, and it is acceptable in quality and form for publication on microfilm and electronically:

_____

_____

_____

_____
Co-Chair

_____
Chair

University of California, San Diego

2014

Dedication

To La Jolla,

Thanks for supporting the beautiful place in 5 years

Table of Contents

List of Figures and Tables

Acknowledgements

I would like to acknowledge to Professor Michael Heller, for all his guidance and assistance to be a creative thinkable scientist over the years. Under his guidance, I could do this whole work. Also, he teaches me that the science is fun.

In addition, I would like to thank Dr. Shaochen Chen for his supporting with the enthusiasm.

To my family and friends in Korea, I want to thank you for whole helping me.

I would like to thank my fellows, who have provided assistance with the creation of this. Especially, I thank Tsukasa Takahasi, Dr. Jennifer Marciniak, Sejung Kim and Yvonne Heneay to endure my irritation as well as be friends

Finally, I want to mention to thank all of scientists and engineers who share their skills and their knowledge in the papers and teach me their tactical knowledge that they are build up at here. Especially, Diether, Ben and Alex who build up this art of work previously in this Lab and Nanogen.

Chapter 1, in part, has been submitted for publication of the material as it may appear in Journal of Nanoscience and Nanotechnology: Youngjun Song, Michael J. Heller “Nanofabrication Using a Micro Scale Electric Field Assembler System for Energy Storage Materials” The dissertation author was the primary investigator and author of this paper.

Chapter 2, in part is a reprint of the material as found in Encyclopedia of Nanotechnology: Youngjun Song, Michae J. Heller “ Electric Field Directed

Assembly of Bioderivatized Nanoparticles": Encyclopedia of Nanotechnology, Springer (2012). The dissertation author was the primary investigator and author of this book chapter.

Chapter 3, in part, is currently being prepared for submission for publication of the materials. Youngjun Song, Yvonne Heaney, Sejung Kim, and Michael J. Heller, Mechanically Strengthen Carbon Nanotubes Networks Flexible Transparent Conductive Electrodes Fabricated by Electrophoretic Deposition. The dissertation author was the primary investigator and author of this material.

Chapter 4, in part, has been submitted for publication of the material as it may appear in Advanced Materials: Youngjun Song, Yvonne Heaney, Tsukasa Takahasi, Sejung Kim and Michael J. Heller, Flexible, Transparent, and Implantable Nitrocellulose Substrates for Electronic Devices. The dissertation author was the primary investigator and author of this paper.

Chapter 5, in part, has been submitted for publication of the material as it may appear in Nature Materials: Youngjun Song, Tsukasa Takahashi, Sejung Kim, Yvonne Heaney, John Warner, Shaochen Chen, Michael J. Heller, A Programmable DNA Double Write Material – Synergy of DNA Photolithography and Self-Assembly Nanofabrication. The dissertation author was the primary investigator and author of this paper.

VITA

2006	Bachelor of Electronics Engineering, Inha University
2006-2008	Flash Memory Development Engineer, Samsung Electronics, Co.
2011	Master of Science, University of California, San Diego
2014	Doctor of Philosophy, University of California, San Diego

PUBLICATIONS

Youngjun Song, Yvonne Heaney, Sejung Kim, and Michael J. Heller, Mechanically Strengthen Carbon Nanotubes Networks Flexible Transparent Conductive Electrodes Fabricated by Electrophoretic Deposition, preparation

Youngjun Song, Yvonne Heaney, Tsukasa Takahasi, Sejung Kim and Michael J. Heller, Flexible, Transparent, and Implantable Nitrocellulose Substrates for Electronic Devices, submitted

Youngjun Song, Tsukasa Takahashi, Sejung Kim, Yvonne Heaney, John Warner, Shaochen Chen, Michael J. Heller, A Programmable DNA Double Write Material – Synergy of DNA Photolithography and Self-Assembly Nanofabrication, submitted

Youngjun Song, Michael J. Heller, Nanofabrication Using a Micro Scale Electric Field Assembler System for Energy Storage Materials, submitted

Youngjun Song, Avery Sonnenberg, Yvonne Heaney, and Michael J. Heller, Device for dielectrophoretic separation and collection of nanoparticles and DNA under high conductance conditions, under review

BOOK CHAPTERS

Youngjun Song, Michae J. Heller “ Electric Field Directed Assembly of Bioderivatized Nanoparticles”: Encyclopedia of Nanotechnology, Springer (2012)

PATENTS

Samsung Q210185, "Thin film deposition apparatus and thin film deposition method using electric field", Jin. S. Heo, Hwi-Yeol Park, Kyung-Hoon Cho, Kyoung-Jwan Choi, Sejung. Kim, Michael J. Heller, Youngjun. Song.

UCSD Disclosure SD2014-003 “Devices, Systems and Processes for Electric Field Directed Self-Assembly NanoFabrication and 3D Heterogeneous Integration and Applications” Michael Heller, Youngjun Song, Sejung Kim.

U. S. patent application for UCSD Case 2013-283 “DNA Double-Write/Double Binding Identity for Micro/Nano Lithography and Self-Assembly Nanofabrication”, Michael Heller, Elaine Skrowronski, Youngjun Song, John Warner, Shaochen Chen.

ABSTRACT

Youngjun Song, Michael J Heller, Nanofabrication on Micro and Macro Scale Electric Field Assembler “Synergy of Top-Down and Bottom-Up Technologies” Electronic Materials and Nanotehnology for Green Enviroment (ENGE) 2014

Michael J. Heller, Youngjun Song, Large Scale Electric Field Array Device for Directed Self-Assembly of Multilayer Nanoparticle Materials, Annual Meeting of the American Electrophoresis Society (AES) 2012

Youngjun Song, Michael J Heller, Nanofabrication on a Macro Scale Electric Field Assembler “Synergy of Top-Down and Bottom-Up Technologies” Electronic Materials and Nanotehnology for Green Enviroment (ENGE) 2012

ABSTRACT OF THE DISSERTATION

Nanoparticles Patterning by Directed Electric Field Assembly

and Photolithography

by

Youngjun Song

Doctor of Philosophy in Electrical Engineering

(Nanoscale Devices and Systems)

University of California, San Diego, 2014

Professor Michael Heller Chair

Professor Yeshaiahu Fainman, Co-Chair

Recently, the integration of a wide range of nanocomponents has been investigated for building patterned or layered structures on the macroscopic and mesoscopic scale. In order to break through the issues of current devices and develop diverse and reliable applications from nanobiomaterials to nanoelectronics, it is necessary to fabricate nano-devices and systems using nanocomponents.

However, traditional fabrication methods have required the modification of these nanomaterials, and need new approaches for the advancement of development for diverse and reliable applications.

In this dissertation, two novel methods are demonstrated for pragmatic nano devices and systems: Controlling extrinsic nanoparticle alignment by electrical field deposition, and intrinsic DNA binding through photolithography.

First, the use of nanoparticles' electrophoretic deposition (EPD) onto porous biodegradable polymer allows the production of transparent flexible carbon nanotube network films with mechanical strength. Most importantly, after solvent treatment, the opaque substrate changed to transparent with conductivity. Thus, we produced flexible transparent films. Another unique aspect of this process is that after solvent treatment, the substrate can be implanted onto newspapers or cloth.

Second, we demonstrate a *DNA double write* process that represents, which allows DNA to be used as a unique material for UV patterning, with subsequent self-assembly via the hybridization of complementary DNA sequences. This novel method allows true synergy for combining top-down photolithography with bottom-up self-assembly. In addition, we have been able to demonstrate both first- and second-level patterning, including target sequence detection and streptavidin /biotin binding with the DNA double write process.

Chapter 1: Introduction

1.1 Introduction

In recently years, nanotechnology has affected diverse research areas, from biology to the electronics industry. For a couple of examples, *in vivo* fluorescent dyes such as quantum dots have been tracked that are sensitive to specific areas (e.g. nucleus, specific proteins, and genes) in cells. Surface Enhanced Raman Spectroscopy (SERS), which enhances Raman scattering by molecules adsorbed on nanostructures, has been used for a surface-sensitive technique of detecting single molecules such as DNA. In particular, the semiconductor industry has predicted that chip performance would double every 18 months, which is called Moore's law. Now, a 15 nm fin field-effect transistor (FET) has been fabricated in industry for high performance systems and low power consumption devices. In non-volatile memory, I participated in developing 32 G bits (45 nm) in 2006 and 64 G bits (32 nm) in 2007, which were recorded on the International Technology Roadmap for Semiconductors (ITRS).

However, industry and science are focused on "More than Moore" (MtM), which has an additional value for devices to improve their functionality beyond the necessarily scale issue. These interests are interested in diverse applications such as biosensors, flexible electrodes, biomedical devices, and other types of semiconductor. To demonstrate these applications, a manufacturing process is needed to develop new assembling technologies and the novel building blocks of nanomaterials. Unlike top-down lithography, the less progress has been made on bottom-up nanoparticle process devices.

This dissertation is primarily focused on the patterning and fabrication of nanocomponents to demonstrate the synergy of top-down and bottom-up technologies. Chapter 1 introduces nanoscience and its applications, summarizes a variety of technologies for nanoparticle assembly, and defines EPD and DNA hybridization. Chapter 2 investigates EPD with addressable layering. Chapter 3 reports on carbon nanotube thin films by EPD for mechanically strong flexible transparent conductive electrodes. Chapter 4 demonstrates transparent and implantable electronic devices for a variety of applications from wearable to paper electronics. Finally, Chapter 5 shows the breakthrough of precision DNA patterning by UV lithography. Thus, in this dissertation, we have focused on nanocomponent patterning and applications using nanoelectronic materials. In addition, we have discussed viable applications using these new methods.

1.2 A variety of methods for nanoparticles assembly

The emergence of nanotechnology over the last few decades shows promise for new approaches to electronic devices and biomedical applications. For example, carbon nanotubes are poised to affect the transistor market, to offer alternative transparent conductive films to replace indium tin oxide, and perhaps enable entirely new electronic structures. Quantum dots have been notably developed for electronic structures such as solar cells, a variety of colored light emitting diodes, and bio-applications such medical imaging and SERS bio-probes. Ultimately, the integration of these nanomaterials, which have been developed for diverse applications with their

unique properties and benefits into large-scale, complex structures needs a new approach or modified fabrication techniques.

The present fabrication techniques can be categorized into two main methods: top-down and bottom-up fabrication. Top-down methods have been developed for semiconductor fabrication methods, and are mostly micro/nanolithography. They include UV photolithography, which is a process used in microfabrication to pattern light-sensitive chemical photoresist through a photomask and electron-beam lithography, which is a process used in nanomanufacturing to draw high resolution shapes on a surface covered with an electron sensitive thin polymer. There are also Steppers, which are used in nano-manufacturing mass production to complete projects rapidly and on a mass-production scale, through a reduction lens and illumination system. Most applications are computer chips, Microfludics devices, and MEMS.

Bottom-up fabrication techniques, which are used to build nanoparticles with a desired nanostructure, are realized through deposition and self-assembly. Common bottom-up fabrication methods include nanoimprint/micro contact printing (MCP), inkjet printing, evaporative-driven self-assembly (EDSA), layer-by-layer (LBL), EPD, and Langmuir-Blodgett (LB). MCP uses micro- or nano- stamps (e.g. PDMS) to pattern materials. Inkjets printing is developed primarily to deposit conductive polymer droplets directly from the print head. EDSA is a technology that drops nanoparticle-loaded solutions that self-assemble during evaporation, and EPD uses electric fields to move particles suspended in a liquid medium between electrodes. LB techniques use the hydrophobic and hydrophilic domains of particular molecules and nanoparticles to assemble a single layer at a time on the designated surface, whereas

other LBL methods use alternating layers of oppositely electrostatically-charged particles/molecules to grow films; it is possible to make heterogeneous LBL.

Nanomaterial self-assembly can be demonstrated in the fabrication of a structure, due to unique material properties, which is arranged into self-assembling monolayers (SAM), DNA linkers, biotin-streptavidin assemblies, nanoparticle surface chemistry, and block copolymers. In this thesis, EPD, LBL and photolithography for nanomaterials are used to show the synergy of top-down and bottom-up technologies.

1.3 Electrophoretic deposition

The EPD method is electrical field deposition for nanoparticles using the charge of the particles in a solution. To avoid electrolysis, normal EPD processes are executed in non-aqueous solutions, but these processes have been demonstrated in high voltage conditions. In this dissertation, the EPD was demonstrated in water-based solutions at lower voltages. In previous work, we have used a microelectronic array device with 400 microelectrodes (with a 55 micron diameter) to carry out electric field–directed (EFD)-LBL assembly of nanoparticles into higher order structures. Using these micro-scale array devices, various DNA, biotin/streptavidin and enzyme derivatized nanoparticles could be fabricated in 55 micron–diameter lift-off structures with up to 40 layers of different nanoparticles.

For high efficiency macro-scale fabrication, we have now designed and fabricated new 4” silicon wafer EFD-LBL devices and micro-size EFD devices. The micro/macro scale EFD-LBL devices are now used to layer micron-sized particles such as lithium cobalt oxide, graphite, and nanoparticles such as carbon nanotubes.

The micro and macro scale EFD-LBL devices and processes have major benefits over conventional LBL self-assembly processes. First, due to the electric field, the particles can be deposited in minutes, which is a rate 100–1000 times faster than classical self-assembly. Second, the EFD-LBL process allows the concentrations of nano/micro-components to be significantly reduced. Third, the integrity of diverse binding reactions between these nano/micro-components, such as electrostatic binding, covalent bonds, DNA pair hydrogen bonds, and antibody-antigen bonds, are maintained throughout the process, granting a vast number of potential material combinations. Fourth, the FD-LBL device allows mask-less patterning with near instantaneous X-Y reconfigurability. Fifth, the final products, fabricated by polymer-coated EFD-LBL platform devices, can be removed via a simple lift-off procedure. EFD-LBL devices represent the true synergy of combining the best aspects of top-down and bottom-up technologies for the heterogeneous integration of diverse and different materials, including combinations of soft-flexible photovoltaic and battery materials for energy harvesting and storage, fuel cells, piezoelectronics, porous coatings and composites, gas diffusion sensors, and substrates for biomedical applications.

1.4 DNA for self-assembly

DNA is a double helix–structure string with Watson-Crick pairing, which can bind two informational strings together. The informational base assembly shows a strong binding property, as the 40 base pairs of 10 nm length have the high melting temperature (~60 °C), which is thermal-dynamically stable. For over a decade, there

have been great expectations regarding novel applications of DNA, ranging from the 3D self-assembly of DNA nanoparticles to DNA nanoelectronic computing. While some of the more biotech-related applications have materialized, most non-classical applications have not. Considering the effort that has been invested in this area, it is disappointing that so little progress has been made.

In this thesis, I demonstrate a DNA double write process that represents a true synergy of combining top-down photolithography and bottom-up self-assembly. This novel method allows DNA to be used as a unique material for UV patterning, with subsequent self-assembly via the hybridization of complementary DNA sequences. Most importantly, after patterned UV exposure to a specially designed DNA write sequence has been immobilized on the substrate, two distinguishable identities are created in the DNA write sequence. Subsequently, two different complementary DNA sequences can now be hybridized in the UV-exposed and unexposed areas. This has not been possible before, and it represents a major attribute not present in other DNA patterning methods. Another unique aspect is that the key to the new process is the special design of the DNA write sequences and the complementary DNA sequences. This means that no chemical modifications of the DNA sequences are necessary to achieve two DNA binding identities. This enabling by DNA sequence design does not preclude the further encoding of large numbers of unique binding identities into the DNA sequences. Thus, the intrinsic programmability of DNA itself is capitalized on to make the DNA material much more useful. Finally, we have been able to demonstrate both first- and second-level patterning with the DNA double write process.

Chapter 1, in part, has been submitted for publication of the material as it may appear in Journal of Nanoscience and Nanotechnology: Youngjun Song, Michael J. Heller "Nanofabrication Using a Micro Scale Electric Field Assembler System for Energy Storage Materials" The dissertation author was the primary investigator and author of this paper.

Chapter 2: Electric Field Directed Assembly of Bioderivatized Nanoparticles

2.1 Overview

Electronic microarray devices which produce reconfigurable electric field patterns can be used to control the self-assembly of nanocomponents into higher order structures. These devices allow the hierarchical assembly of nanocomponents to be carried within microscale geometries of electronic circuitry. Such nanofabrication devices and technologies have the potential for producing highly integrated nano/ micro/macrostructures including nanophotonic-based large-scale arrays and displays; high-efficiency multiple band gap photovoltaics; fuel cells with nanostructured intermetallic catalysts and integrated fluidic channeling; smart-morphing nanocomposite materials; in vivo biosensor and mother-ship drug delivery devices. Electronic microarray devices that were originally developed for molecular diagnostic applications allow DNA, proteins, and almost any charged nanostructure to be rapidly transported and specifically bound at any site on the array surface. Microarray devices that have onboard integrated CMOS circuitry also allow rapid switching and precise control of the currents/voltages sourced to the microarray. Such microarray devices have been used to carry out the rapid highly parallel assisted self-assembly of biotin- and streptavidin-derivatized fluorescent nanoparticles and DNA-derivatized nanoparticles into multilayer structures. Electric field–directed assembly has major advantages over more classical passive layer-by-layer (LBL) self-assembly processes, which are generally one order of magnitude slower, nonparallel, and not reconfigurable in real time. The use of electronic microarray devices for assisted self-

assembly represents a unique synergy of combining the best aspects of “top-down” and “bottom-up” technologies into a potentially viable nanomanufacturing process. It also enables a more bio-inspired logic to be followed for the hierarchal self-assembly of nanostructures into higher order structures, materials, and devices.and “bottom-up” technologies into a potentially viable nanomanufacturing process. It also enables a more bio-inspired logic to be followed for the hierarchal self-assembly of nanostructures into higher order structures, materials, and devices.

2.2 Nanotechnology Top-Down and Bottom-Up Processes

Nanotechnology includes a wide range of new ideas and concepts that are likely to enable novel applications in electronics, photonics, materials, energy conversion processes, biosensors, and biomedical devices. Some of the many challenges and opportunities in nanotechnology were discussed in the early National Nanotechnology Initiative meeting. One of the more important challenges is the area of nanofabrication, in particular the development of technologies which will lead to cost-effective nanomanufacturing processes. Enormous efforts are now being carried out on refining the more classical “top-down” photolithography processes to produce silicon- integrated (CMOS) electronic devices with nanometer scale features. While this goal has been achieved, the process requires billion dollar fabrication facilities and it does appear to be reaching some fundamental limits. So-called bottom-up self-assembly processes are also being studied and developed as possible new ways for producing nanodevices and nanomaterials. While there are now numerous examples of promising nanocomponents such as organic electron transfer molecules, quantum dots,

carbon nanotubes, and nanowires, their assembly into higher order structures has been limited. Thus, the development of a viable cost-effective bottom-up self-assembly nanofabrication process that allows billions of nanocomponents to be assembled into a higher order structure still remains a considerable challenge.

2.2.1 Living System and DNA Self-assembly

Living systems represent the best example of self-assembly processes that can be used for developing strategies for bottom-up nanofabrication. Living systems contain many types of biomolecules which have high fidelity recognition properties including deoxyribonucleic acid (DNA), ribonucleic acid (RNA), and proteins. Proteins serve as structural elements (collagen, keratin, silk, etc.), as binding recognition entities (antibodies) and as efficient catalytic macromolecules (enzymes). The nucleic acids DNA and RNA are involved in the storage and transfer of genetic information. All these biomolecules are able to interact and organize into higher order nanostructures which translate genetic information and perform biomolecular syntheses and energy conversion metabolic processes. Ultimately, all these biomolecules and bionanostructures are integrated and organized within membrane structures to form the entities called cells. Cells in turn can then replicate and differentiate (via these nanoscale processes) to form and maintain living organisms. Thus, biological systems have developed the ultimate “bottom-up” nanofabrication processes that allow component biomolecules and nanostructures with intrinsic self-assembly and catalytic properties to be organized into highly intricate living organisms. Of all the different biomolecules that could be useful for nanofabrication,

the nucleic acids (DNA and RNA) with their high fidelity recognition and intrinsic self-assembly properties represent a most promising material for creating nanoelectronic, nanophotonic as well as many other types of organized nanostructures. DNA, RNA, and other synthetic DNA analogues are programmable molecules which through their base sequence have intrinsic molecular recognition and self-assembly properties. Short DNA sequences, called oligonucleotides, are readily synthesized by automated techniques and can be modified with a variety of functional groups such as amines, biotin moieties, fluorescent or chromophore groups, and with charge transfer molecules. Additionally, synthetic DNA molecules can be attached to quantum dots, metallic nanoparticles, carbon nanotubes; as well as to surfaces like glass, silicon, gold, and semiconductor materials. Synthetic DNA molecules (oligonucleotides) represent an ideal type of "Molecular Legos" for the self-assembly of nanocomponents into more complex two- and three-dimensional higher order structures. At a first level, DNA sequences can be used as a kind of template for assembly on solid surfaces. The technique involves taking complementary DNA sequences and using them as a kind of selective glue to bind other DNA-modified macromolecules or nanostructures together. The base pairing property of DNA allows one single strand of DNA with a unique base sequence to recognize and bind together with its complementary DNA strand to form a stable double-stranded DNA structures. While high fidelity recognition molecules like DNA allows one to "self-assemble" higher order structures, the process has some significant limitations. First, for in vitro applications (i.e., in a test tube), DNA and other high fidelity recognition molecules like antibodies, streptavidins, and lectins work most efficiently when the complexity of the system is

relatively low. That is as the complexity of the system increases (more unrelated DNA sequences, proteins, and other biomolecules), the high fidelity recognition properties of DNA molecules are overcome by nonspecific binding and other entropy-related factors, and the specific hybridization efficiency for the DNA molecules is considerably reduced. Under in vivo conditions (inside living cells), the binding interactions of high fidelity recognition molecules like DNA are much more controlled and compartmentalized, and the DNA hybridization process is assisted by structural protein elements and active dynamic enzyme molecules. Thus, new bottom-up nanofabrication processes based on self- assembly using high fidelity recognition molecules like DNA should also incorporate strategies for directing and controlling the overall process.

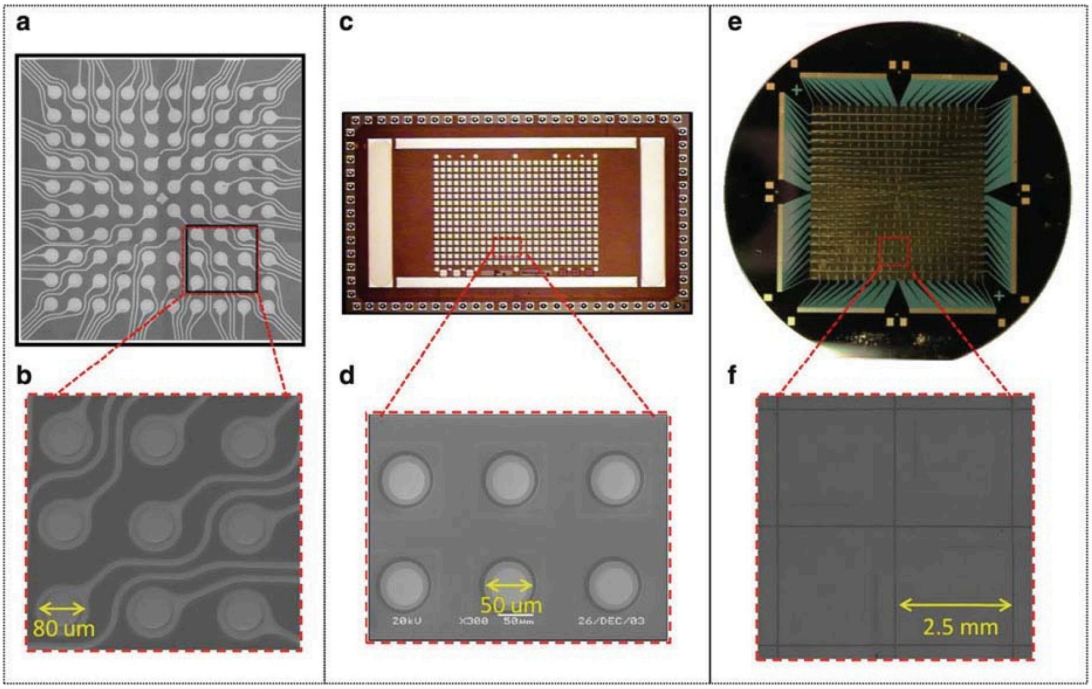

Figure 2.1 Three different array devices for electric field–directed nanoparticle assembly. (a) View of a 100 test-site microarray device with 80 µm diameter platinum microelectrodes, the device is approximately 5 X 5 mm in size. (b) A close-up of the 80 µm microelectrodes. (c) A 400 test-site CMOS electronic microarray device with 50 µm diameter platinum microelectrodes and four perimeter counterelectrodes, the device is approximately 5 X 7 mm in size. (d) A close-up of the 50 µm diameter microelectrodes. (e) A 400 silicon wafer size electric field–directed assembler device. The total active deposition area is 5 cm^2 with 200 platinum electrodes which are 2.5 X 2.5 mm with 8 mm gaps. (f) Shows a close-up of four of the electrodes

2.2.2 Electronic Microarray DNA Hybridization Technology

A variety of electronic microarrays have been designed and fabricated for DNA genotyping diagnostic applications. An early 100 test-site electronic microarray which has been commercialized (Nanogen) has an inner set of 80 µm diameter platinum microelectrodes (Fig. 2. 1a, b). Each microelectrode has an individual wire interconnect through which current and voltage are applied and regulated. The microarrays are fabricated from silicon wafers, with insulating layers of silicon dioxide, platinum microelectrodes, and gold connecting wires. Silicon dioxide/silicon

nitride is used to cover and insulate the conducting wires, but not the surface of the platinum microelectrodes. The whole surface of the microarray is covered with several microns of hydrogel (agarose or polyacrylamide) which forms a permeation layer. The permeation layer is impregnated with streptavidin which allows attachment of biotinylated DNA probes or other entities. The ability to use silicon and microlithography for fabrication of the DNA microarray allows a wide variety of devices to be designed. More sophisticated higher density electronic microarrays with 400 test-sites have on-chip CMOS control elements for regulating the current and voltages to the microelectrode at each test-site (Fig. 1c, d). These control elements are located in the underlying silicon structure and are not exposed to the aqueous samples that are applied to the chip surface when carrying out the DNA hybridization reactions. DNA hybridization reactions are carried out on these electronic microarrays by first applying a positive DC bias of ~ 2– 4 V to address or spot specific DNA molecules to the selected test-sites on the array. These DNA molecules are usually oligonucleotide "capture" probes or target DNA sequences that have been functionalized with biotin molecules. These biotinylated DNA molecules become strongly bound to streptavidin molecules which are cross-linked to the hydrogel layer covering the underlying microelectrode. In the next step, a positive DC electric field is applied to specific microelectrodes directing the hybridization of the other DNA molecules to the DNA sequences attached to the selected test-sites. (During the addressing and hybridization processes, other microelectrodes on the microarray are biased negative.) Electronic addressing also allows DNA probes to be spotted onto the array in a highly reproducible manner. Electronic microarrays can be formatted in a

variety of ways that include reverse dot blot format (capture/identity sequences bound to test-sites), sandwich format (capture sequences bound to test-sites), and dot blot format (target sequences bound to test-sites). DNA hybridization assays involve the use of fluorescent DNA reporter probes designed to hybridize to specific target DNA sequences. The reporter groups are usually organic fluorophores that have been either attached to oligonucleotide probes or to the target/sample DNA/RNA sequences. After electronic addressing and hybridization are carried out, the microarray is analyzed using the fluorescent detection system. Gilles P.N. et al., Nature Biotechnology 17(4), 365-370 (1999) provides a good example of single nucleotide polymorphism (SNP) genotyping analysis that has been carried out on using electronic microarrays.

2.3 Electric Field–Directed Nanofabrication

While electronic microarray devices were originally developed for DNA genotyping diagnostic applications, the resulting electric fields are able to transport any type of charged molecule or structure including proteins, antibodies, enzymes, nanostructures, cells, or micron-scale devices to or from any of the sites on the array surface. In principle, these active devices serve as a “mother-board” or “host-board” for the assisted assembly of DNA molecules or other entities into higher order or more complex structures. Since the DNA molecules have intrinsic programmable self-assembly properties, and can be derivatized with electronic or photonic groups, or attached to larger nanostructures (quantum dots, metallic nanoparticles, nanotubes), or microstructures, this provides the basis for a unique bottom-up nanofabrication process. Thus, electronic microarray devices can serve as motherboards that allow one

to carry out a highly parallel electric field “pick and place” process for the heterogeneous integration of molecular, nanoscale, and micron-scale components into complex three- dimensional structures. Electric field–directed self-assembly technology is based on three key physical principles: (1) the use of functionalized DNA or other high fidelity recognition components as “Molecular Lego” blocks for nanofabrication; (2) the use of DNA or other high fidelity recognition components as a “selective glue” that provides intrinsic self-assembly properties to other molecular, nanoscale, or micron- scale components (metallic nanoparticles, quantum dots, carbon nanotubes, organic molecular electronic switches, micron and submicron silicon lift-off devices and components); and (3) the use of an active micro- electronic array devices to provide electric field assistance or control to the intrinsic self-assembly of any modified electronic/photonic components and structures.

2.3.1 Electric Field–Directed Self-assembly of Bioderivatized Nanoparticles

In addition to the more classical top-down processes such as photolithography, so-called bottom-up processes are being developed for carrying out self-assembly of nanostructures into higher order structures, materials, and devices. To this end, considerable efforts have been carried out on both passive and active types of layer-by-layer (LBL) self-assembly processes as a way to make three-dimensional layered structures, which can have macroscopic x-y dimensions. In cases where patterned structures are desired, the substrate material is generally pre-patterned using masking and a photolithographic process. Other approaches to patterning include the use of

optically patterned ITO films and active deposition of the nanoparticles. Nevertheless, limitations of passive LBL as well as active assembly processes provide considerable incentive to continue the development of better paradigms for nanofabrication and heterogeneous integration. Of particular importance to self-assembly processes involving biomolecular-derivatized nanoparticles is the prevention of nonspecific binding. Nonspecific binding due to cooperative hydrophobic, hydrogen bonding and ionic interactions between nanoparticles and the assembly substrate may often be as strong as the specific ligand binding interactions. Thus, once a nanoparticle has been bound nonspecifically, it is often difficult to remove it without perturbing or damaging the more specific nanoparticle interactions and structures. Nonspecific binding is often a concentration-dependent problem, whose probability increases when large amounts of derivatized nanoparticles interact with a physically and/or chemically complex substrate. Alternatively, trying to carry out stringent self-assembly at very low concentrations of biomolecular-derivatized nanoparticles is a slow process, and may still result in nonspecific binding to unprotected areas of the substrate. Therefore, there is a clear need for a rapid, directed assembly process which utilizes low concentrations of nanocomponents and reduces nonspecific interactions throughout the repeated multistep processes that will be required for fabricating complex higher order structures.

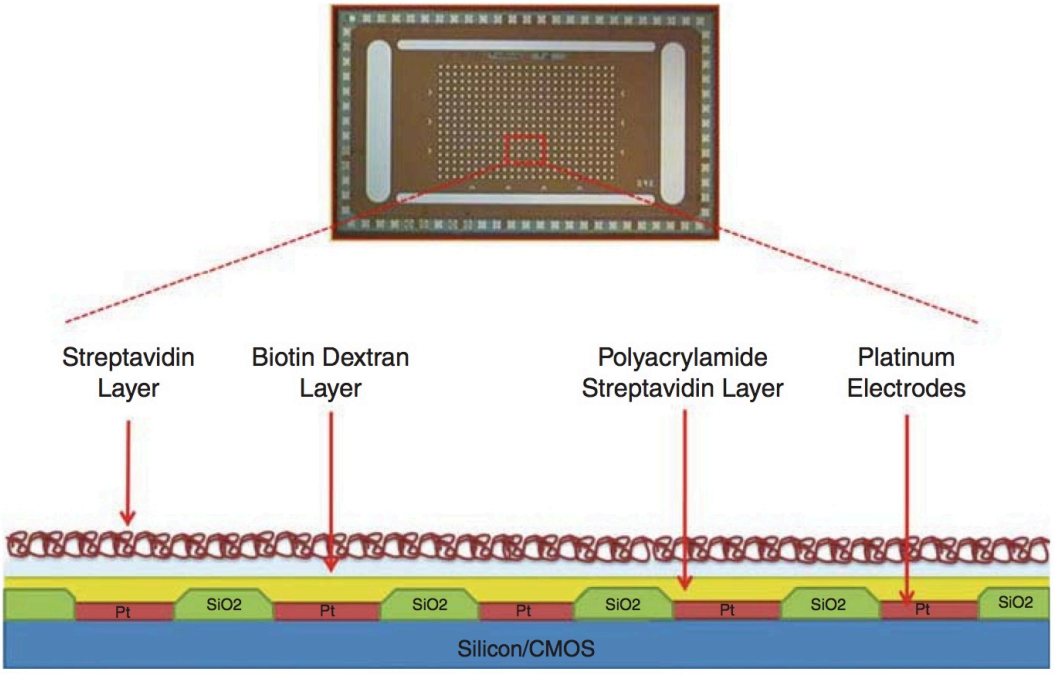

Figure 2.2 The 400 test-site CMOS electronic microarray device. The 400 test-site device, with a cross- sectional diagram showing the silicon base, the CMOS control circuitry, the platinum microelectrodes, the silicon dioxide insulating structures between the microelectrodes, the overlaying polyacrylamide/streptavidin permeation gel layer, the biotin–dextran layer, and the final layer of streptavidin (the drawings are not to scale)

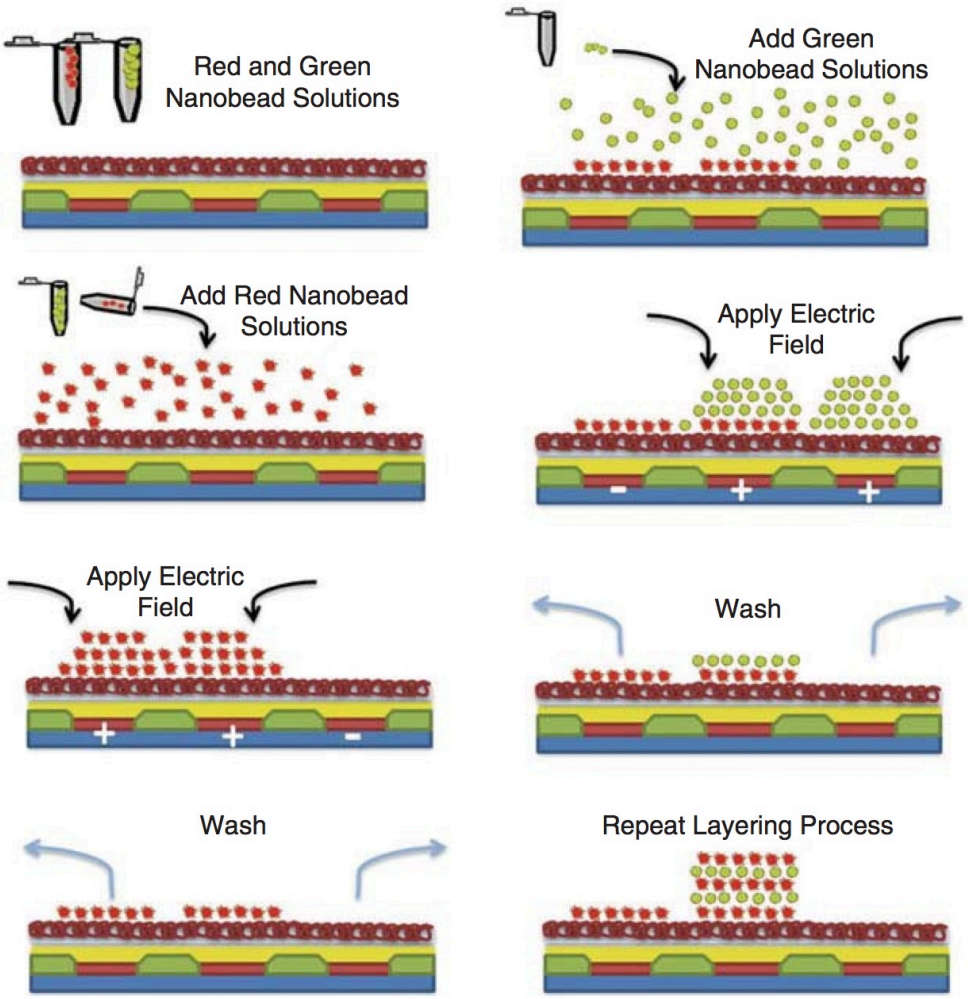

Figure 2.3 The electric field–directed nanoparticle layering process. The initial step involves adding a solution containing the biotinylated 40 nm red fluorescent nanoparticles onto the microarray device. The next step involves applying a positive DC biased to the desired test-sites on the microarray which attracts and concentrates the negatively charged biotinylated nanoparticles to the surface. The biotinylated nanoparticles become bound to the streptavidin layer, and the unattached nanoparticles are then washed away. In the next step, a solution containing streptavidin 40 nm yellow-green fluorescent nanoparticles is placed onto the microarray; the positively biased test-sites on the microarray attract and concentrate the negatively charged streptavidin nanoparticles which now become bound to the biotinylated nanoparticle monolayer. The unattached nanoparticles are then washed away. The alternate addressing, binding, and washing of biotin and streptavidin nanoparticles are repeated to form the multilayer nanoparticles structures

2.3.2 Electronic Microarrays and Techniques

Electronic microarrays and electric field techniques have now been used to carry out the highly parallel directed self-assembly of biomolecular-derivatized nanoparticles into multilayered higher order structures. The rapid and highly parallel assembly of biotin-, streptavidin-, and DNA-derivatized nanoparticles into structures with over 40 layers has been achieved. The optimized electric field process allows nanoparticles at very low concentration in the bulk solution to be rapidly concentrated and specifically bound to the activated sites with minimal nonspecific binding. The electric field device used to obtain such results was an ACV 400 CMOS electronic microarray (Nanogen). This CMOS-controlled electronic micro- array contains 400 50 μm diameter platinum micro- electrodes in a 16 X 25 grid arrangement (Fig. 2. 1c). The device has four additional large rectangular counterelectrodes on its perimeter. Each of the 400 microelectrodes is capable of independently producing from 0 to 5 V at up to 1 mA per microelectrode. The 400 microelectrodes on the array can be biased positive, negative, or left neutral in basically any combination; however, all four of the perimeter electrodes must be biased at the same polarity (positive or negative) or left neutral. The electronic microarray device can be set to source either current or voltage, and the activation time for each microelectrode can be controlled independently. The microarray device uses platinum electrodes as they present an inert interface to the solution. Additionally, the platinum electrodes do not degrade or disintegrate from the electrolysis reactions which occur at the voltages (>1.2 V) necessary to produce rapid electrophoretic transport of nanoparticles in the bulk solution. The ACV 400 site microarray comes coated with a 10 μm thick (hydrated) porous permeation layer

composed of polyacrylamide impregnated with streptavidin (Fig. 2. 2). This permeation layer is designed to prevent analyte molecules (DNA, proteins, etc.) and nanoparticles from contacting the microelectrodes, and to ameliorate the adverse effects of the electrolysis products on the binding reactions. In order to improve nanoparticle binding density, the microarray surface was overlayered with a biotin–dextran layer and a high density streptavidin layer (Fig. 2. 2). The basic scheme for the electric field–directed self-assembly of biotin and streptavidin nanoparticles is shown in Fig. 2. 3, and a full description of the actual procedure is given in Dehlinger D.A. et al., Nano Letter 8 4053-4060 (2008).

2.3.3 Procedure for Deposition of First Nanoparticle Layers

The microarray is first washed with a 100 mM solution of L-histidine to remove any excess streptavidin. The bulk of the liquid on the chip is then removed, and 20 mL of a 4 nM solution of biotinylated 40 nm red fluorescent nanoparticles in 100 mM L-histidine buffer is deposited onto the micro- array surface. Because most of the derivatized nanoparticles used in the experiments have a net negative charge, microelectrodes used for deposition are biased positive, with the outer perimeter counter- electrodes being biased negative. A number of micro- electrodes on the array are often left unbiased (not activated) and served as overall controls for non- specific binding. Immediately after addition of the nanoparticle containing solution, the directed electrophoretic transport and deposition of nanoparticles to the specific array sites is carried out. In initial experiments, the microarray can be set up in a combinatorial fashion to test a variety of currents, voltages, and activation times to

determine optimal deposition conditions. Generally, a current ramp from 0 to 0.4 mA in 0.025 mA increments is programmed along rows of microelectrodes on the array. Activation times from 0 to 20 s in 5 s intervals are programmed across groups of columns on the microarray. Several columns of microelectrodes are also left inactivated to serve as controls. Following directed electrophoretic transport of the biotinylated 40 nm nanoparticles, the microarray is washed six times with 100 mM L-histidine, and then all liquid is removed from the microarray to prevent crystallization of the histidine upon drying.

2.3.4 Procedure Multilayer Nanoparticle Depositions

The basic combinatorial directed deposition procedure is repeated in order to determine optimal conditions (current, voltage, and activation time) for producing best quality alternating layers of biotin and streptavidin nanoparticles. Template experiments can be used for determining nanoparticle layering conditions (which could be run on the same microarray in highly parallel manner). The first template experiment involves alternating the deposition of biotin 40 nm red fluorescent nanoparticles and streptavidin 40 nm yellow-green fluorescent nanoparticles in a grid type format. In this format, groups of columns of microelectrodes are set to different activation times (typically between 0 and 30 s), and the rows of micro- electrodes are set to different current levels (0.025–0.4 mA in 0.0.025 mA increments). Several repeats of the combinatorial pattern are done across the whole microarray, and intervening columns of microelectrodes are left inactivated to serve as controls. This combinatorial approach allows for a relatively quick determination of the optimal time

and current conditions necessary to achieve the best deposition and layering. A second type of template experiment is used to determine the level of self-adhesion (nonspecific binding) between similar nanoparticles (biotin to biotin and streptavidin to streptavidin). This is carried out by having regions on the microarray only activated on alternate deposition cycles, when the same type of nanoparticle solution is exposed to the microarray. This experiment tests if the same type of nanoparticle would accumulate without the presence of its specific ligand binding partner. In these experiments, a single column per template is activated during every deposition to serve as a positive control for biotin-to-biotin nanoparticle binding and streptavidin-to-streptavidin nanoparticle binding. Additional columns of microelectrodes are not activated throughout the experiment, and serve as overall controls for more general nonspecific binding to the microarray. All of these experiments are monitored in real time and imaged by an epifluorescent microscope set at 540 nm emission for the yellow- green fluorescent nanoparticles and 610 nm emission for the red fluorescent nanoparticles. Imaging was carried out using a Hamamatsu Orca-ER camera.

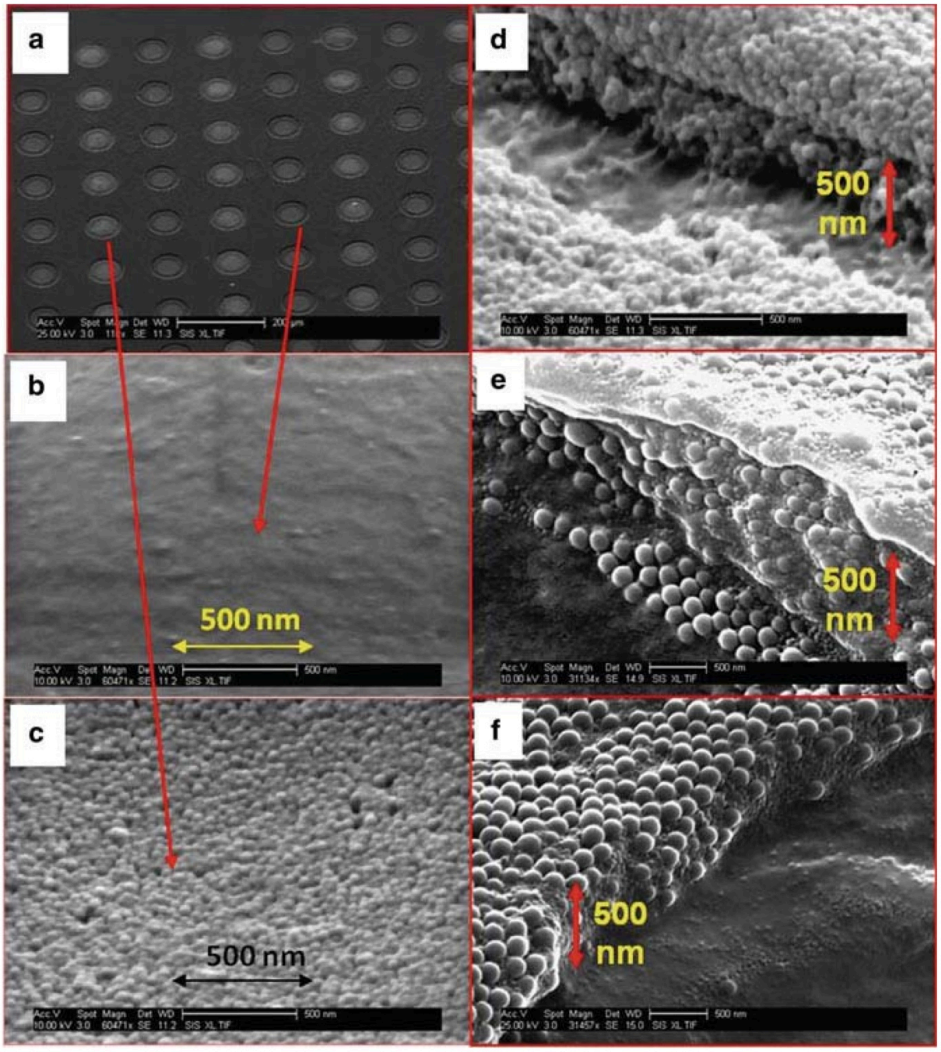

Figure 2.4 Results of electric field–directed nano- particle assembly/layering on a microarray device. (a) Shows a section of the 400 site CMOS microarray device where alternate rows of microelectrodes were used to carry out nanoparticle layering. Rows with bright circular spots had 40 layers of alternating 40 nm red fluorescent biotin nanoparticles and 40 nm green fluorescent streptavidin nanoparticles deposited by applying a DC electric field. Rows with lighter circular spots had no electric field applied. (b) Shows an SEM image of a microelectrode which had no DC field applied. No nanoparticles have been deposited. (c) Shows a SEM image of a microelectrode to which the DC electric field was applied. Nanoparticles have been deposited on this surface. (e) Shows an SEM image of a cross section of a 40 layer structure of alternating 40 nm red fluorescent biotin nanoparticles and 40 nm green fluorescent streptavidin nanoparticles. (f) Shows an SEM image of a cross section of a 40 layer structure of alternating 40 nm biotin nanoparticles and 200 nm streptavidin nanoparticles. (g) Shows another SEM image of a cross section of a 40 layer structure of alternating 40 nm biotin nanoparticles and 200 nm streptavidin nanoparticles

2.3.5 Multilayer Biotin–Streptavidin Nanoparticle Structures

One of the main advantages of the electric field–directed self-assembly fabrication process is the ability to direct the streptavidin–biotin ligand binding to only occur on the specific microelectrodes which have been positively biased. Figure 2. 4a shows a section of the 400 site CMOS microarray device where alternate rows of microelectrodes were used to carry out biotin–streptavidin nanoparticle layering. Rows with bright circular spots had 40 layers of alternating 40 nm red fluorescent biotin nanoparticles and 40 nm yellow- green fluorescent streptavidin nanoparticles deposited by applying a DC electric field. Rows with lighter circular spots had no electric field applied. Figure 2. 4b shows a scanning electron microscope (SEM) image of a microelectrode which had no DC field applied. It can clearly be seen that no biotin nanoparticles have bound to this surface, despite the fact that it contains a streptavidin binding layer and has been exposed to the biotin nanoparticles 20 times. Figure 2. 4c shows an SEM image of a microelectrode to which the DC electric field was applied. Nanoparticles have clearly been deposited on this surface. Multilayer nanostructures were verified by using SEM to image fractured cross sections of the 40 layer structures of alternating 40 nm red fluorescent biotin nanoparticles and 40 nm green fluorescent streptavidin nanoparticles (Fig. 2. 4d). In other work, multilayer layers structures containing alternating 40 nm biotin nanoparticles and 200 nm streptavidin nanoparticles were fabricated. Figure 2. 4e, f show the SEM image of cross sections of 40 layer structure of alternating 40 nm biotin nanoparticles and 200 nm streptavidin nanoparticles.

Multilayer DNA Nanoparticle Structures – In other work, electric field–directed hybridization was used to produce 20 layer nanostructures composed of DNA- derivatized nanoparticles. Using the same CMOS electronic microarray device, DNA nanoparticles could be directed and concentrated such that rapid and specific hybridization occurs only on the activated sites. Nanoparticles layers were formed within 30 s of activation, and 20 layer structures were completed in under an hour. The results of this work carry significant implications for the future use of DNA nanoparticles for directed self-assembly nanofabrication of higher order structures. Advantages for using electric field directed fabrication of DNA nanoparticles include the following: First, the electric field process for the directed hybridization of DNA nanoparticles was significantly faster than the passive process; second, the electric field–directed process requires the use of only minimal concentrations of DNA nanoparticles, which would not be viable for passive hybridization process which requires much higher concentration of nanoparticles; third, the integrity of the biomolecular binding reactions (hybridization) and the ionic flux was maintained throughout the large number of process steps (20 depositions). Thus, high fidelity DNA hybridization and a large number/variety of unique DNA binding sequences can be used for nanofabrication; fourth, the higher order layered DNA nanoparticle structures can ultimately be removed from the microarray by a relatively simple lift-off procedure. Thus, an electric field array device can serve as a manufacturing platform for making higher order 3D structures; and fifth, the overall process demonstrated the nanofabrication of higher order structures from a relatively heterogeneous group of materials, that is, biotin–dextran polymers, streptavidin, and

two different sets of DNA nanoparticles.

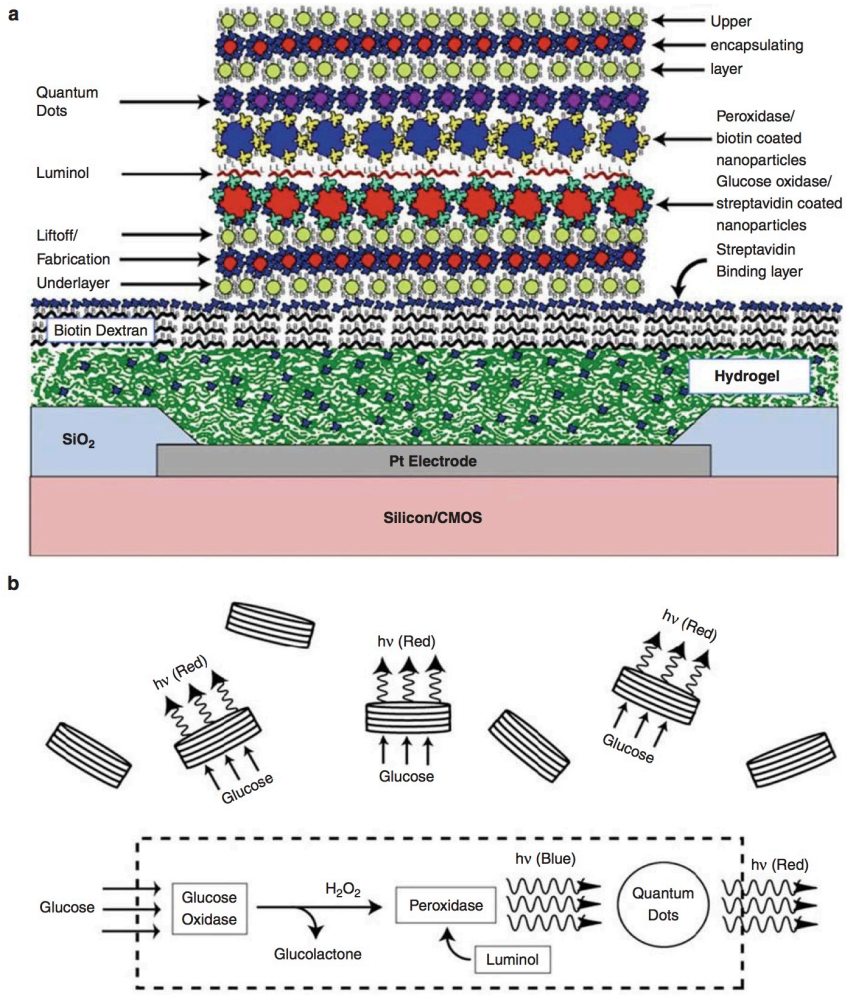

Figure 2.5 Future glucose micro-biosensor device fabricated by electric field–directed assembly. (a) The basic glucose micro-biosensor structure would include a bottom (lift- off) layer of biotin–streptavidin nanoparticles; a layer of glucose oxidase–streptavidin nanoparticles; a layer of luminol–dextran– biotin; a layer of streptavidin, a layer of peroxidase–biotin nanoparticles, a layer of red fluorescent streptavidin quantum dots, and a final upper capping layer of biotin–streptavidin nanoparticles. (b) When placed in a sample containing glucose, the glucose would diffuse into the micro-biosensor device and react with the glucose oxidase to produce hydrogen peroxide. The hydrogen peroxide and luminol diffusing to the peroxidase layer would catalyze the chemiluminescence (blue light). The blue light via fluorescent energy transfer to red fluorescent quantum dots would now produce detectable red fluorescence signal

2.4 Future Work

Some important potential future applications for the electric field–directed nanofabrication process include miniaturized chemical and biosensor devices, "micron-sized" dispersible chemo/biosensors for environmental and bioagent detection, lab-on a-chip devices, and in vivo diagnostic/drug delivery systems. Figure 2. 5 shows the scheme for a future glucose micro- biosensor device fabricated using electric field–directed nanoparticle assembly. The basic glucose micro- biosensor structure would include a bottom (lift-off) layer of biotin–streptavidin nanoparticles; a layer of glucose oxidase–streptavidin nanoparticles; a layer of luminol–dextran–biotin; a layer of streptavidin, a layer of peroxidase–biotin nanoparticles, a layer of red fluorescent streptavidin quantum dots, and a final upper capping layer of biotin–streptavidin nanoparticles. When placed in a sample containing glucose, the glucose would diffuse into the micro-biosensor device and react with the glucose oxidase to produce hydrogen peroxide. The hydrogen peroxide and luminol diffusing to the peroxidase layer would catalyze the chemiluminescence (blue light). The blue light via fluorescent energy transfer to red fluorescent quantum dots would now produce detectable red fluorescence signal. This demonstrates that different fluorescent color responses could be created. Electronic array devices have other advantages including that they can be designed in a wide variety of shapes and sizes. To this end, larger "macroarray" devices have now been fabricated which can produce layered nanostructures with macroscopic dimensions. Figure 2. 1e, f show a 4 in. silicon wafer size electric field array device. The total active deposition area for this device is 5 cm^2 with 200 platinum electrodes which are 2.5 x 2.5 mm with 8mm gaps. Such

“macroarray” devices will have applications for producing advanced fuel cells and photovoltaic materials. Overall electric field–directed nanofabrication using electronic array devices represents a unique synergy of combining the best aspects of “top-down” and “bottom- up” technologies into a viable nanofabrication process. It also represents a bio-inspired logic for self-assembly and hierarchal scaling of nanocomponents into integrated microscopic structures.

Chapter 2, in part is a reprint of the material as found in Encyclopedia of Nanotechnology: Youngjun Song, Michae J. Heller “ Electric Field Directed Assembly of Bioderivatized Nanoparticles”: Encyclopedia of Nanotechnology, Springer (2012). The dissertation author was the primary investigator and author of this book chapter.

Chapter 3: Mechanically Strong Carbon Nanotube Networks with Flexible Transparent Conductive Electrodes Fabricated by Electrophoretic Deposition

3.1 Introduction

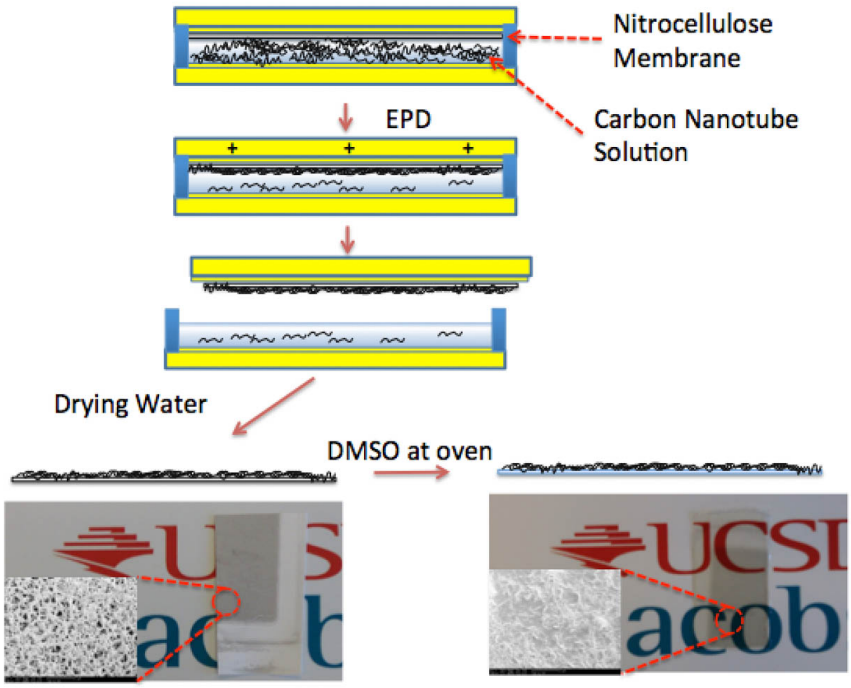

Figure 3.1 Summary of scheme and images of transparent electrode

Self-assembly is a powerful method for scalable uniform fabrication and consistent performance of nanoparticles onto flexible transparent substrates. Several methods of self-assembly have been investigated such as Langmuir-Blodgett, nano-imprinting, printing and filtration, but for a truly scalable method, electrical field deposition or electrophoretic deposition methods have the upper hand over other methods for several reasons: the ability to control a deposition thickness of self-

assembled nanoparticles by the strength of the electrical field, minimal concentration usages, fast fabrication time, and the ability to deposit a diverse range of materials from biomaterials to electronics components at low cost. These benefits were investigated by *Ammam et al.*, who researched glucose oxidase deposition by asymmetrical alternating current (AC) electrical field, *Hsiao et al.*, who researched layered nanoparticles and the glucose oxidase structure using electric-field-directed self-assembly layer-by-layer technology, *Chang et al.*, who researched proteins and DNA patterned by direct current (DC) electrical fields and their ability to transfer materials onto an insulated polymer, and *Edman et al.* and *O'Riordan et al.*, who researched an electrical field self-assembled mesoscale solid state based light emitting diode (50μm diameter, 11μm thickness). Remarkable benefits aside, the drawback of traditional electrophoretic deposition methods is the need for it to be executed on non-transparent metal electrodes into the solution. To produce transparent conductive electrodes (TCEs) by electrophoretic deposition, *Lima et al.* used carbon nanotube deposition onto metal electrodes coated glass. Afterwards, the metal was etched to produce the transparent electrodes. Unfortunately, for the flexible substrates, this process has a drawback that the metal etchant can be degraded the transparent insulated substrates, which primarily consist of polymer plastic materials, such as polyethylene-naphthalate (PEN) films and polyethylene terephthalate (PET) films. Here, we demonstrate that a network of carbon nanotubes can be fabricated onto a nitrocellulose membrane by electrophoretic deposition to produce flexible TCEs. Through solvent wetting and evaporation processes, the carbon nanotube network films can become transparent while maintaining conductivity. (Figure 3.1) This

process allows the nitrocellulose-based carbon nanotube flexible TCEs to be mechanically strong because nitrocellulose materials, which have a binding property, can fix carbon nanotube networks onto the surface from the carbon nanotube network laid free stranding that have mechanically weak binding.

3.2 Experimental Section

3.2.1 Conductive nanoparticle deposition by electrical field

A cleaned 3 x 2 inch glass slide was deposited with Ti/Au (50/200 nm) using a Denton Discovery 18 Sputter System. A 0.5 mm plastic wall that was cut by a laser-cutting machine was attached using double-sided pressure sensitive adhesive tape on the 3 x 2 inch electrode. 0.2 μm pore size nitrocellulose paper was attached with water on the top electrode. Afterwards, trapped bubbles were taken out using the plated glass slide between the top electrode and the nitrocellulose membrane (Bio-Rad, Inc.). The solution of conductive nanoparticles was poured in the bottom electrode well and the top electrode with nitrocellulose paper was put on the top electrodes. After the electrodes were connected with wires, voltage was applied between the top and bottom electrodes for 30 seconds.

3.2.2 Preparation of carbon nanotube solution

CVD single wall carbon nanotubes were purchased from Cheap Tube, Inc. and arc-discharged single wall carbon nanotubes were purchased from Sigma-Aldrich Corp. and CMC (9,000 MW) was purchased from Sigma-Aldrich Corp.. These two

carbon nanotubes were mixed with 10:1 ratio of CMC:DI water and sonicated for 2 hours. The solution was used only from the top 75 % of the tube.

3.2.3 Nitrocellulose transparent procedure

First, conductive nanoparticles were deposited onto NC paper and dried in an oven at 85^{o}C for 5 minutes or room temperature overnight. DMSO was dropped on a substrate plate and the conductive nitrocellulose membrane was laid on the substrate carefully to make the membrane transparent. The sample was dried in an oven at 85^{o}C for 1 hour.

3.2.4 Measurement of transmittance, sheet resistance, SEM

Transmittance values of the films were measured using a uv-vis spectrometer (PerkinElmer, Inc.). The samples were placed flat outside of the sample holder and scanned from 850 to 300 nm. The films were measured by the Jandel four-point probe with RM 3000 test (Jandel, Inc.) at multiple points and averaged to give the final sheet resistance values. The morphology of the films was recorded on the Phillips XL30 ESEM operating at 3 kV.

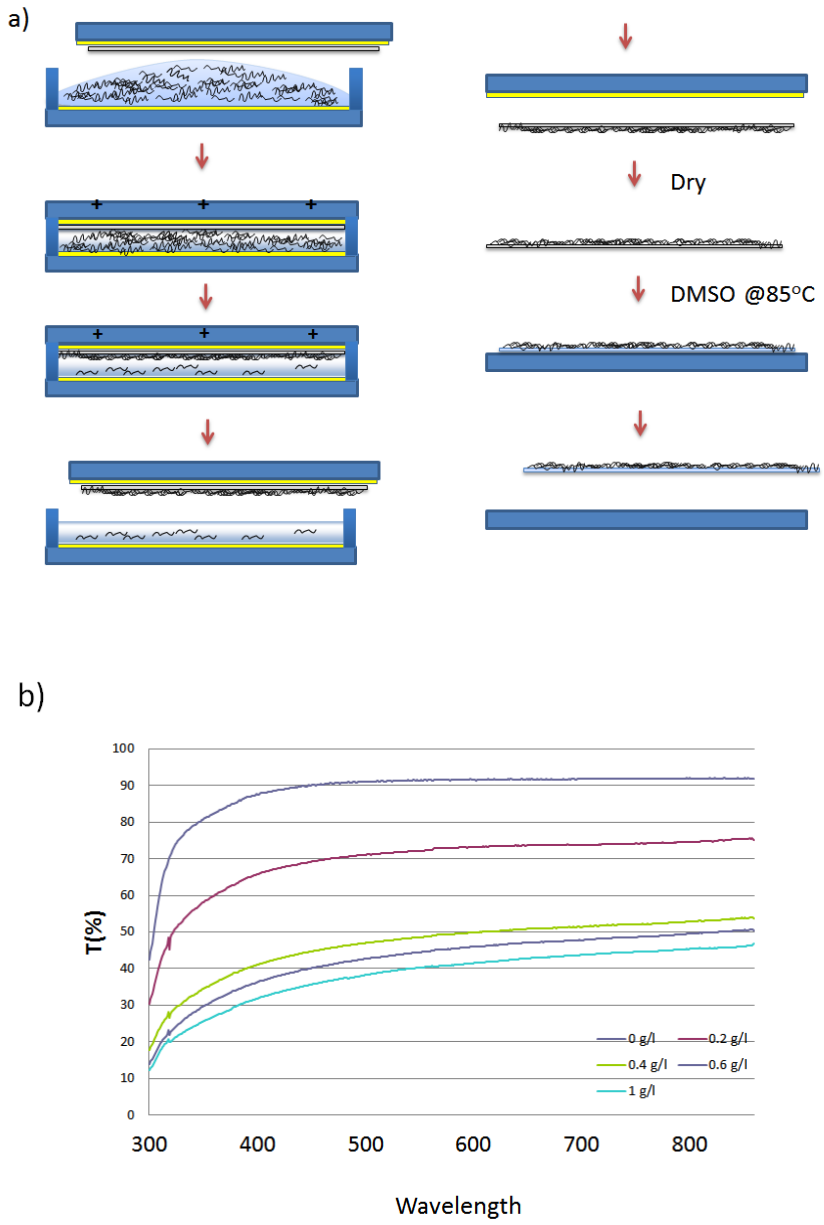

Figure 3.2 Scheme of fabrication process and graph of transmittance a) scheme of the fabrication process; step 1 is to pour the solution and cover the top electrode with water to activate the nitrocellulose membrane, step 2 is to apply the voltage (top electrode is 2.5 V, bottom electrode is 0 V), step 3 is the deposition of carbon nanotubes onto the nitrocellulose membrane surface, steps 4 and 5 are to remove the top electrode take and lift off the carbon nanotube-deposited nitrocellulose, step 6 is the first drying process and step 7 is second drying process after DMSO treatment ; b) graph of transmittances by EPD for different concentrations.

3.3 Results and Discussion

For the electrophoretic deposition process and the fabrication of uniform carbon nanotube networks, a uniform charged membrane substrate that can be constantly bound electrostatically and a device that has even electrical fields for electrophoretic deposition are necessary. To create a positively charged membrane surface, the nitrocellulose membrane was coated with a positively charged poly-L-lysine. Then, the negatively charged carbon nanotubes, wrapped with carboxymethyl cellulose (CMC) as a surfactant, were deposited onto the positively charged nitrocellulose membrane surface by electrophoretic deposition. To carry out this process, two different electrodes and a chamber are required: the top gold electrode serves as a layering nitrocellulose membrane that is the deposition site and the bottom gold electrode that works with the chamber to contain the carbon nanotube suspension. Figure 3. 2a shows the detailed process for flexible transparent conductive electrode fabrication by electrophoretic deposition. After activating the poly-L-lysine coated membrane with water, the membrane was laid onto the top electrode with no air bubbles, which can produce defects (non-deposition of carbon nanotubes) on the surface. A single wall carbon nanotube suspension was poured into the bottom electrode chamber. Once the top electrode with the nitrocellulose membrane was mounted in parallel onto the chamber wall of the bottom electrode, DC voltage (2.5 V) was applied across the electrodes for 30 seconds and then the top electrodes were detached from the chamber. After being lifted off, the nitrocellulose membrane deposited with carbon nanotubes was dried in the oven (85°C) for 5 minutes or at room temperature overnight. Next, a dimethyl sulfoxide (DMSO) evaporation process

was used to make the nitrocellulose membrane transparent: After the DMSO was applied on the uniform glass slide or the wafer substrate, the nitrocellulose membrane was laid onto the substrate, with the carbon nanotube networks facing up. After the DMSO was allowed to evaporate in the oven (85°C) for 1 hour, the carbon nanotube network nitrocellulose film became transparent while maintain the networks onto the film surface. Finally, the dried film that was detached from the substrate became TCE with transparency and flexibility.

For the uniform carbon nanotube network fabrication without increasing sheet resistance, we optimized two main processes. First, to optimize the electrophoretic deposition process, we investigated the parameters such as the applied voltage and the deposition time. At a high voltage (>2.5 V), we saw undeposited areas due to bubbles between the electrode and the nitrocellulose membrane. At a low voltage (<1 V), we saw a significant decrease in the amount of carbon nanotube deposition onto the nitrocellulose membrane. To reach fast fabrication without any significant bubble effects, we fixed the electrophoretic deposition conditions at 2.5 V for 30 seconds. In 30 seconds, most carbon nanotubes in suspension were deposited onto the nitrocellulose surface and constructed the carbon nanotube network, which has a dominant effect on sheet resistance values. Second, to fix the value of sheet resistance, it is necessary to control the amount of DMSO applied to the substrate in the step that make the film transparent. Because the solvent evaporation process of DMSO leads to decomposition and reconstruction of the membrane structure, the amount of DMSO used is very critical for carbon nanotube networks to stay on the surface of the

membrane. If the DMSO amount is copious, the carbon nanotube network becomes embedded inside the nitrocellulose membrane while drying. Implanting the carbon nanotube network significantly increases its sheet resistance value. This is not only due to the disappearance of the carbon nanotube network on the surface, but the carbon nanotubes also lose their adsorption between one another inside the nitrocellulose film. It is a well known fact that surfactants and polymers increase the sheet resistance value because the polymer blocks the carbon nanotube network. The effect of carbon nanotube networks wrapped in diverse polymers with cellulose were reported by *Li et al.*, and *Chang et al.* developed PVDF- carbon nanotube films that can obtain constant-stress extension regions in stress-strain tests, compared with typical low-extensibility feature of neat PVDF film.

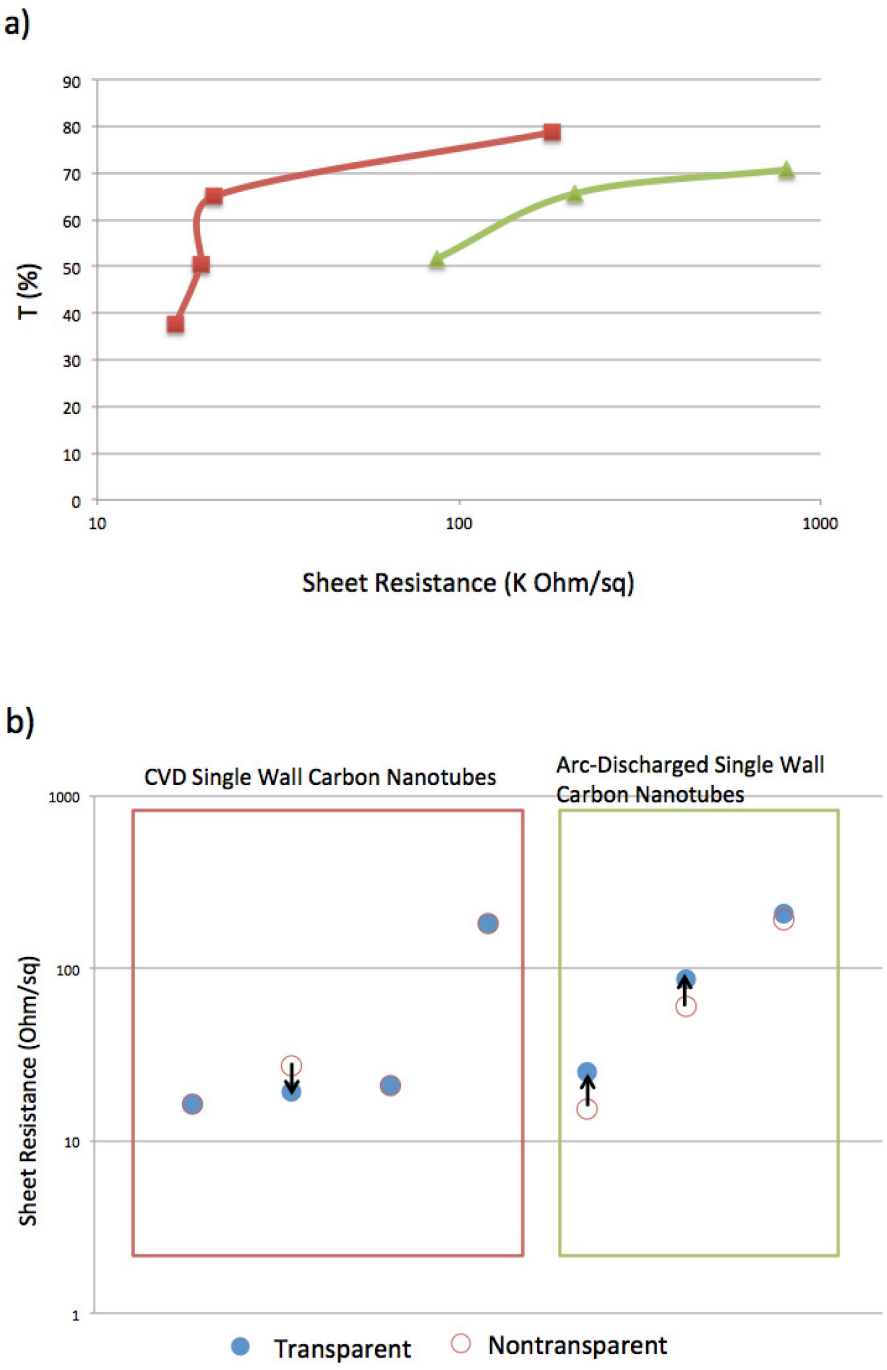

Figure 3.3 The graphs of transmittance of transparent conductive electrodes a) Transmittance vs. sheet resistance (red: CVD single wall carbon nanotube, green: Arc-discharge single wall carbon nanotube); b) Results of sheet resistance values from the DMSO treatment process.

Figure 3.2b shows the relationship between solution concentrations for electrophoretic deposition (2.5V, 0.5mm distance between anode and cathode) and the transmittance of final product of our fabrication method. The transmittance for the nitrocellulose membrane without carbon nanotube network is 91.43 % at 550 nm. However, the carbon nanotubes deposited nitrocellulose membranes with DMSO treatment have different transmittances depending on the carbon nanotube solution concentrations. Since the solution concentration increased, the transmittance was decreased in the final product. The film deposited a 0.2 g/L concentration solution which dramatically decreased transmittance to 72.14 % at 550 nm. The film deposition of 0.4 g/L has 48.58 % transmittance. This is because with electrophoretic deposition, the higher concentration of carbon nanotubes encrusts higher density of the networks, which blocks more light from transmitting onto the transparent nitrocellulose film (91.43 % at 550nm shown in figure 3.2b). Therefore, the films that contain a higher density of carbon nanotube networks have lower transmittance values than lower density carbon nanotube networks. Thus, the relationship of transmittance value and conductivity of the carbon nanotube TCEs is a trade-off. This is due to the high density carbon nanotube networks with lower transmittance have more electrical pathway through the carbon nanotube networks, but the low density carbon nanotube networks with the higher transmittance have fewer electrical connections. To investigate a more detailed relationship between transmittance and conductivity for this method, we show the correlation graph of sheet resistance value verses transmittance in figure 3.3a. The transmittance and the sheet resistance values of CVD single wall carbon nanotubes were measured and are shown in figure 3.3a (red line).

The cases of arc-discharged single wall carbon nanotubes were measured and are shown in figure 3.3a (green line).

The sheet resistance values were not changed after the DMSO treatment process (figure 3.3b; blue dots) compared to the values before the treatment (figure 3.3b; red dots). The values of arc-discharge single wall carbon nanotube networks were slightly increased, but not significantly; in fact, most values were consistent and some of the CVD single wall carbon nanotube network values had decreased. Because CMC was wrapped on the carbon nanotubes, the sheet resistance values of carbon nanotubes mixed with CMC is higher than the pristine carbon nanotube networks values such as a normal free standing carbon nanotube network. However, this free standing carbon nanotube network for electrodes is expected to be bound weakly. In this research, we focused on electronics, but the benefits can extend to optical devices such as displays and more. In those cases, we can use a higher amount of DMSO.

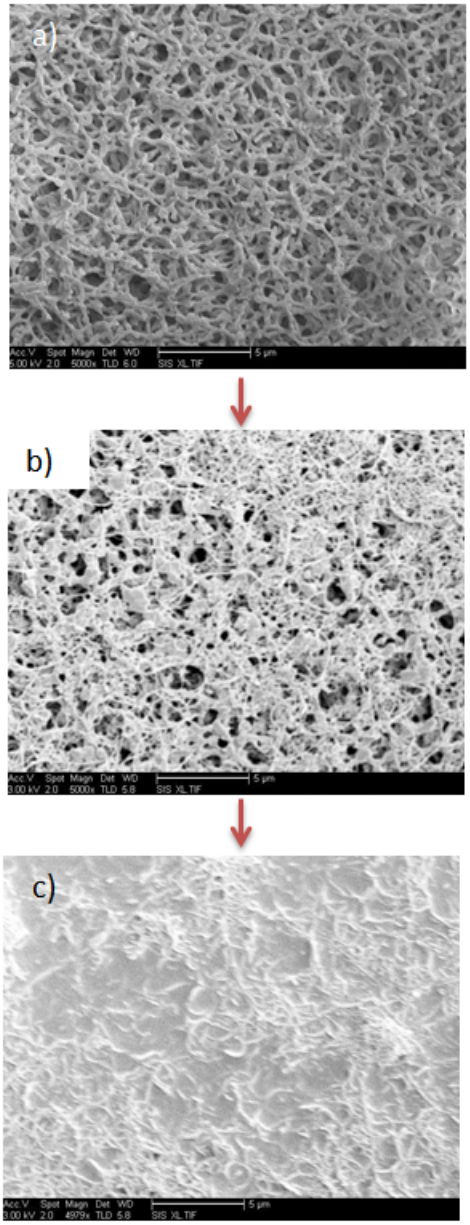

Figure 3.4 SEM images a) Polymer SEM; b) Conductivity SEM; c) Conductivity transparent SEM

To see the morphology change for this membrane during the process, we monitored the surface by scanning electron microscopy (SEM). The original nitrocellulose coated with poly-L-lysine had the smallest (200 nm) and largest (1 µm) pores that can be used for electrophoretic deposition of carbon nanotube nanoparticles.

Poly-L-lysine had no effect on morphology because the nitrocellulose membrane was coated with 1% poly-L-lysine to cover the whole porous surface. However, the poly-L-lysine function allows the negatively charged nitrocellulose surface to become a positively charged surface, which makes electrostatic bonding of negatively charged carbon nanotubes with CMC easy. The thickness of the carbon nanotube network is 10 to 20 nm, and the length of the carbon nanotubes range from 10 to 50 µm. The largest carbon nanotube network deposited onto the nitrocellulose substrate is shown in Figure 3.4b. Finally, after the DMSO-evaporated treatment, the carbon nanotubes deposited nitrocellulose membrane was transparent with pores removed and the carbon nanotube network wrapped by the cellulose.

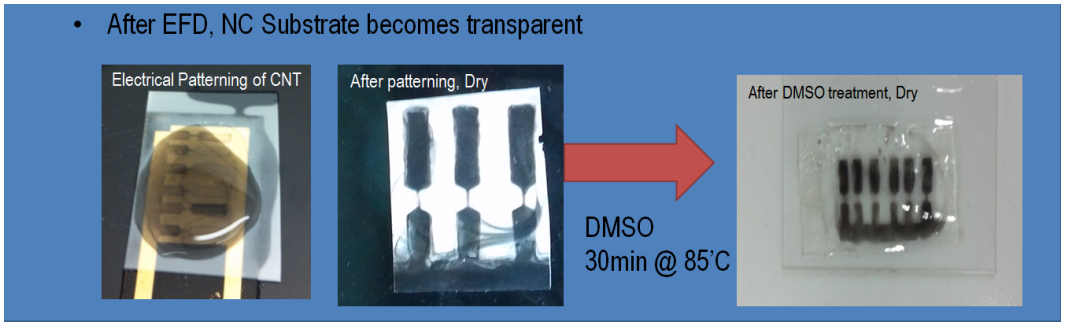

Figure 3.5 Pattern deposition of carbon nanotubes onto nitrocellulose by electrophoretic deposition

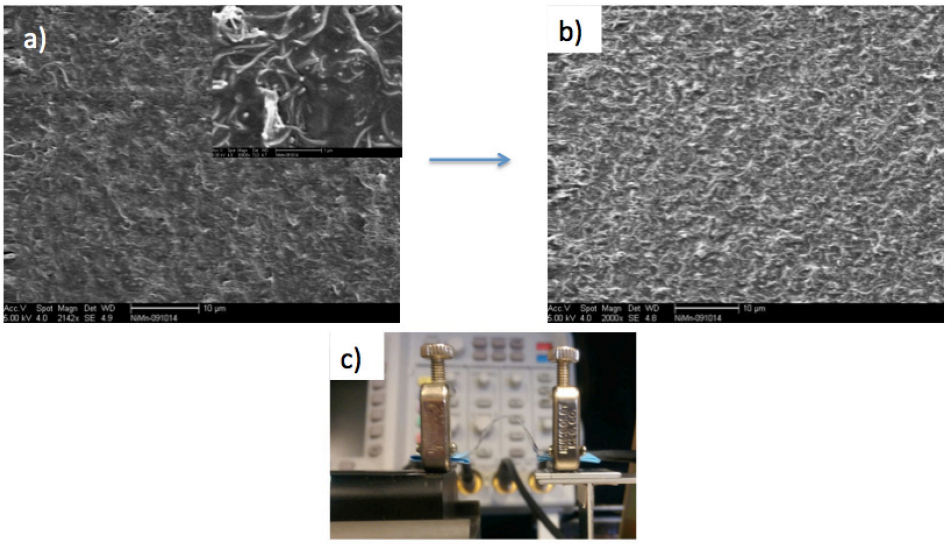

Figure 3.6 SEM images after flexible endurance test (4.7K times) a) before bending test b) after bending test c) image of bending test

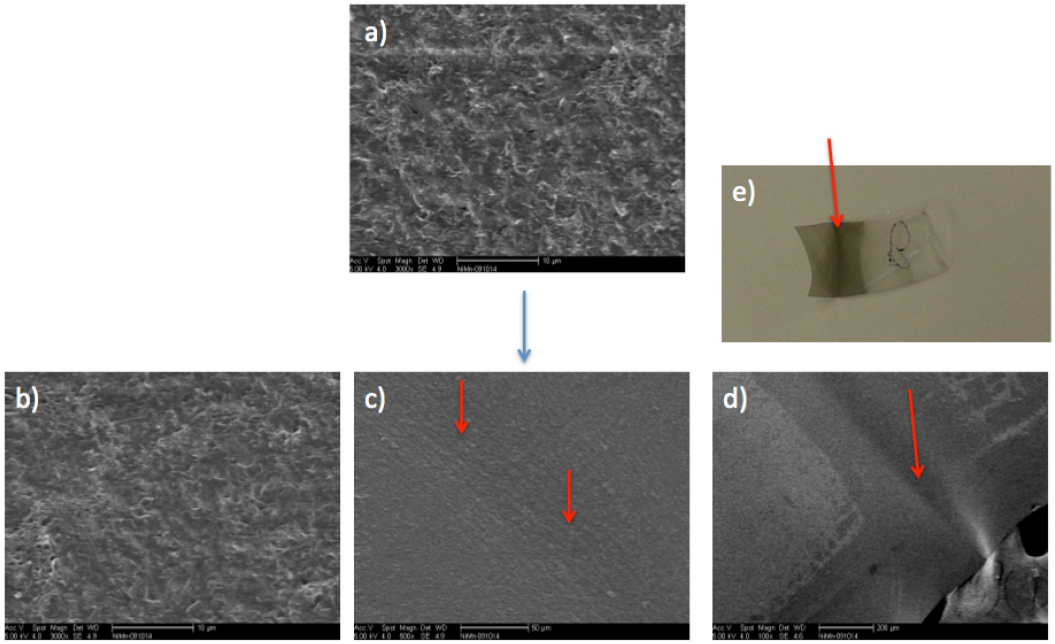

Figure 3.7 SEM image of folding test a) before folding test b), c), d) and e) after folding test

Recently, flexible transparent substrates using cellulose materials were researched actively because they are simple cellulose fiber extracts from wood that are cheap, abundant and environmentally friendly. *Nogi et al.* reported a transparent cellulose paper for the first time in 2009. *Okahisa et al.* used this substrate for flexible organic light-emitting diode displays in the same year. The group from the University of Maryland reported the use of these cellulose substrates and various optoelectronics such as transparent organic field-effect transistors and solar cell enhancing materials. *Koga et al.* then researched that for transparent electronics, carbon nanotube networks and silver nanowire networks deposited onto transparent cellulose paper by filtration compared with normal PET film by drop casting. However, these substrates still have weakness against water or air sensitive electronic materials such as conductive polymers due to the porous paper structure. Our non-porous cellulose based film device with carbon nanotube networks attached by electrophoretic deposition and solvent treatment has several benefits: (1) water resistance, which has strong benefits for electronic devices, (2) air stability, which is useful for lithium ion batteries or polymer device, (3) patterning of nanoparticles (figure 3.5.), and (4) mechanical strength after DMSO evaporation process. This is because carbon nanotubes are now permanently fixed on the substrate by nitrocellulose that is worked as binding materials after the nitrocellulose treatment by DMSO evaporation. To test mechanical endurance, we demonstrate 4700 times bending and 180^{o} folding in half. After bending, there is no distinguishing between before bending and after bending status shown in figure 3.6. There are a small number of wrinkles where it has been folded, but there is no disconnection onto edge lines (figure 3.7).

3.4 Conclusion

In summary, we demonstrated a new approach for electrophoretic deposition, which has become an attractive method for novel coating or films of carbon nanotubes , using the porous nitrocellulose membrane as the thin and flexible substrate. During the process, the membrane became transparent and the pores vanished through the solvent treatment during which the nitrocellulose was melted and reconstructed. Also, we showed that the nitrocellulose functions as a binder, which can fix carbon nanotubes strongly on the substrate. This process also has the benefit of being able to control the transmittance and sheet resistance values through a diverse range of suspension concentrations. This method and flexible TCEs can be applied to many diverse applications. We believe this method has benefits in thin flexible transparent applications such as solar cells, OLEDs and touch screens. This method also allows for patterning of nanoparticles such as quantum dots (QDs) or biomolecules.

Chapter 3, in part, is currently being prepared for submission for publication of this material. Youngjun Song, Yvonne Heaney, Sejung Kim, and Michael J. Heller, Mechanically Strengthen Carbon Nanotubes Networks Flexible Transparent Conductive Electrodes Fabricated by Electrophoretic Deposition. The dissertation author was the primary investigator and author of this material.

Chapter 4: Flexible, Transparent, and Implantable Nitrocellulose Substrates for Electronic Devices

4.1 Introduction

The unique properties of lightweight, flexible, transparent, and thin substrates have played a key role in daily life such as newspapers. However, integrating electronics directly with paper substrates have significant challenges due to surface morphology of these materials that have roughness and porous structures. In order to break through this limitation, we investigated a uniform, adhesive, and transparent polymer substrate that can be combined with diverse materials with electronic and optical properties.

Here, we demonstrate transparent nitrocellulose films that have diverse transmittances after treatment with solvents, as well as nanoparticle deposition, metal sputtering deposition, and dye processing for optical filters. Using this nitrocellulose membrane, we demonstrate a 17 Ω/sq transparent conductive electrode consisting of a network of flexible silver nanowire (AgNW) that has been successfully implanted onto newspaper without losing conductivity. The reason why this research can be carried out is the unique properties of nitrocellulose, which can be made transparent with solvent by and melting and re-forming it.

Commonly, nitrocellulose has been used for a long time to carry out a diverse range of application in many areas, after it was discovered by Christian Friedrich Schonbein and Rudolf Christian Bottger between 1845-1847. In the biology field, the nitrocellulose membrane can be used as a Western-blotting substrate for transferring protein. In the commercial industry, it is well known that a nitrocellulose solvent

solution can been used as a lacquer that coats materials on woods such as furniture to form a protective layer. Also, nitrocellulose film was used in photography film. Recently, cellulose fiber was researched as a substrate for transparent conductive electrodes for optoelectronics. However, this membrane constructed by cellulose fibers mesh has weaknesses for the passivation of electrostatics, water, and air due to the porosity in the membrane and the integration with other flexible substrates due to its binding properties. In this study, we introduce a nitrocellulose substrate applied using various fabrication methods: (1) a conductive, transparent, and implantable AgNW network using electrophoretic deposition, (2) laser printing using a paper-like property, (3) shadow masking metal sputtering deposition, (4) spraying of carbon nanotubes and (5) dying for optical filters. The nitrocellulose substrate deposited AgNW and/or laser-printed methods can use for optoelectronics because the opaque porous substrate can be changed to a transparent uniform substrate without any pores when it is melted and reconstructed by solvent treatment. Finally, we show that this AgNW network is successfully embedded onto newspaper and cloth using the backside of the nitrocellulose, which can be used to attach adhesive materials.

4.2 Experimental Section

4.2.1 Fabrication of transparent nitrocellulose electrode

For the electrophoretic deposition, the metal electrode composed of Ti/Au (50 nm/ 200 nm) was sputtered onto a cleaned glass slide (3 x 2 inch.) via directly current (DC) magnetron sputtering (Denton Vacuum Discovery 18 system). Then, a plastic wall with 0.5 mm of thickness as a spacer was attached to the bottom electrode used as an anode using double-sided pressure sensor tape (PST) on the metal electrodes in

order to contain AgNWs suspension. The porous nitrocellulose paper (NC papers) with 0.2 mm pore size (Bio-Rad, Inc.) activated with poly-L-lysine was applied to the top electrode used as a cathode and then, AgNWs solution was poured into the fabricated cathode. The electrodes were mounted in a parallel-plate configuration with a gap of 0.5 mm. The DC bias was applied by a DC power supply across the electrodes for 30 seconds, and the current that flowed through the suspensions during the deposition was measured.

4.2.2 Transparent process

Once AgNWs were deposited on the NC papers and dried using an oven at 85 ^{o}C for 3 minutes, DMSO was dropped on the dried SWCNTs/NC on a substrate plate in order to make it transparent. The sample was dried in an oven at 85 ^{o}C for 1 hour.

4.2.3 Laminating of nitrocellulose electrode

DMSO was sufficiently dropped onto newspapers and garments to wet fully. Afterwards, AgNW/NC laid onto wet newspapers and garments. And the sample was dried in an oven at 85 ^{o}C for 3 hours.

4.2.4 Characterization and measurement

To measure the transmittance, a UV-vis spectrometer (PerkinElmer, Inc.) was used from 300 to 850 nm with an incident angle of 90º. The sheet resistance of the SWCNTs/NC paper film was measured by the Jandel four probes with RM 3000 test (Jandel, Inc.) at multiple points and averaged to get the final sheet resistance value. The morphology of the films was recorded on Phillips XL30 ESEM operating at 10 kV.

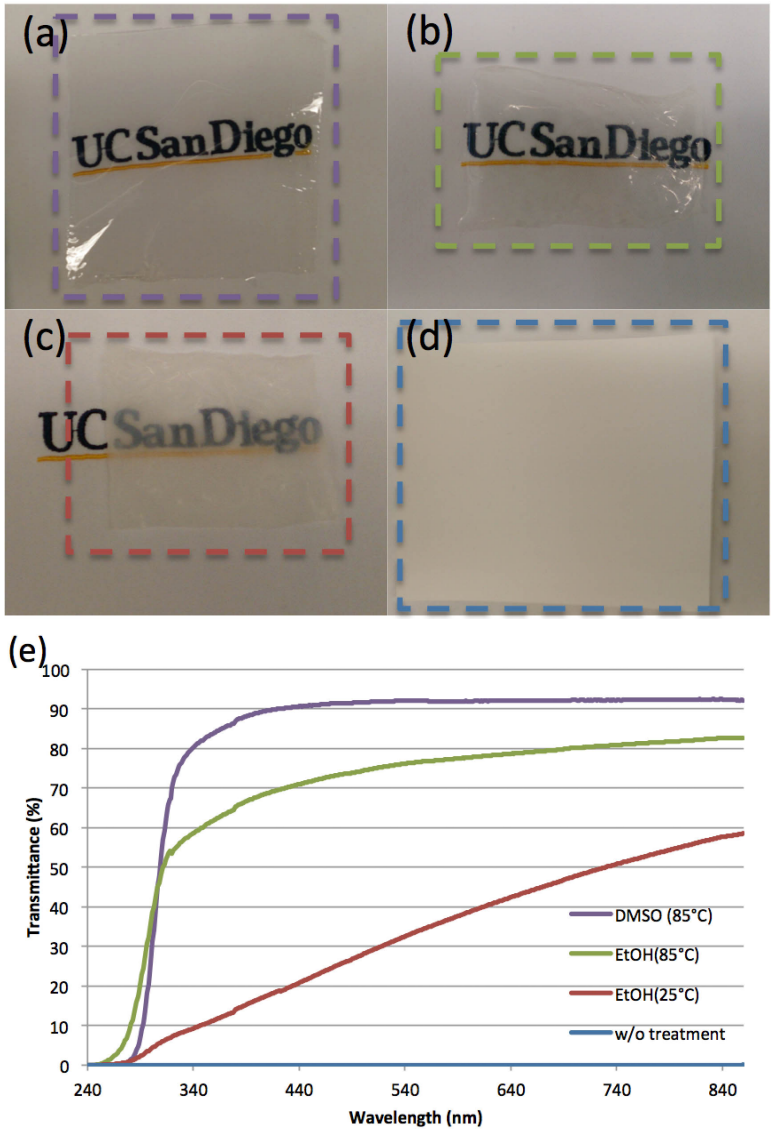

Figure 4.1 Transparent nitrocellulose films: (a) 92% transmittance by DMSO treatment at 85 ^{o}C, (b) 75% transmittance by ethanol treatment at 85 ^{o}C, (c) 32% transmittance by ethanol treatment at room temperature, (d) 0% transmittance without treatment; (e) Transmittance graph

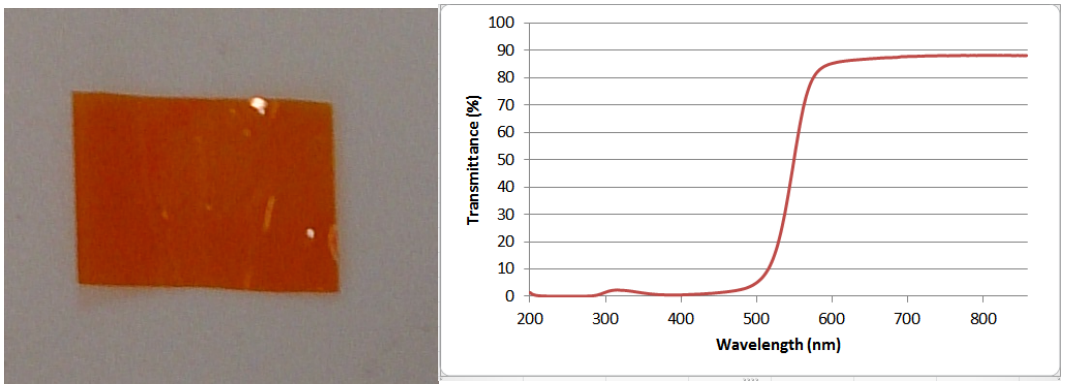

Figure 4.2 Optical image and uv-vis results of Sudan II dye onto nitrocellulose

4.3 Results and Discussion

In figure 4.1, we demonstrate that the nitrocellulose substrates, which are normally used for protein transferring called Western-blotting, were fabricated into transparent films that have difference transmittances after different solvent treatments. We found several benefits of this substrate for use as a fabrication method and in electronics devices; (1) a pristine porous substrate that can deposit nanoparticles by electrophoretic deposition, (2) an insulated material which can be used for electronic device, (3) diverse transmittances by several solvent treatments and evaporation conditions, (4) flexibility, and (5) easy to attach to other materials such as paper or cloth. Using the different solvents and drying conditions, the opaque nitrocellulose substrate had varying diverse transmittance values. After wetting with dimethyl sulfoxide (DMSO) and drying in an oven at 85 ^{o}C, the nitrocellulose substrate was made transparent, as shown in figure 4.1a, and has a 92% transmittance value at 540 nm (Fig. 4.1e; purple line). Through 100% ethanol treatment, transparent films with two different transmittance values were obtained depending on temperature; 76% (Fig. 4.1e; green line) at 85 ^{o}C, 32.5% (Fig. 4.1e; red line) at 25 ^{o}C. However, in the case of

ethanol containing any fraction of water such as 95% ethanol (5% DI water), the substrate could not change the transmittance value. The nitrocellulose substrate treated with ethanol containing water reverted to its original opaque status during the drying process. Using the same substrate and this time treating it with DMSO, the substrate achieved transparency. We think the water functions to disturb the nitrocellulose melting by the solvents. Because this substrate has a high uniform transmittance after solvent evaporation, from 360 to 860 nm, it demonstrates an optical long-pass filter. The nitrocellulose substrate was dye-doped by Sudan II which is used for PDMS optical long-pass filters. The optical long-pass filter is described in Supporting Information (Fig. 4.2).

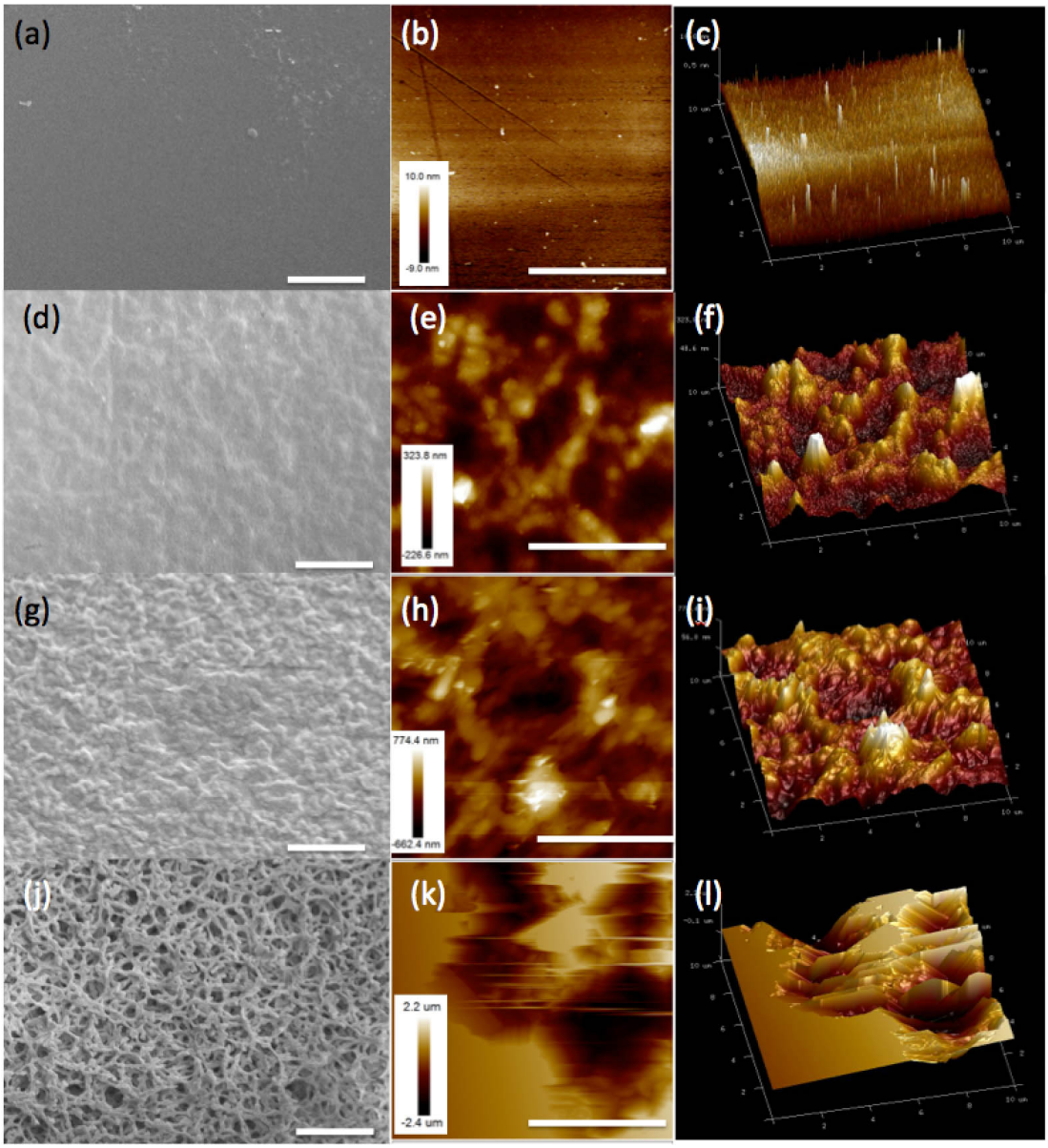

Figure 4.3 SEM and AFM images of nitrocellulose (a)-(c) nitrocellulose after DMSO treatment (d)-(f) 7 nitrocellulose after EtOH treatment at 85 ^{o}C (g)-(i) nitrocellulose after EtOH treatment at room temperature (j)-(l) pristine nitrocellulose. Scale bars are 5 µm.

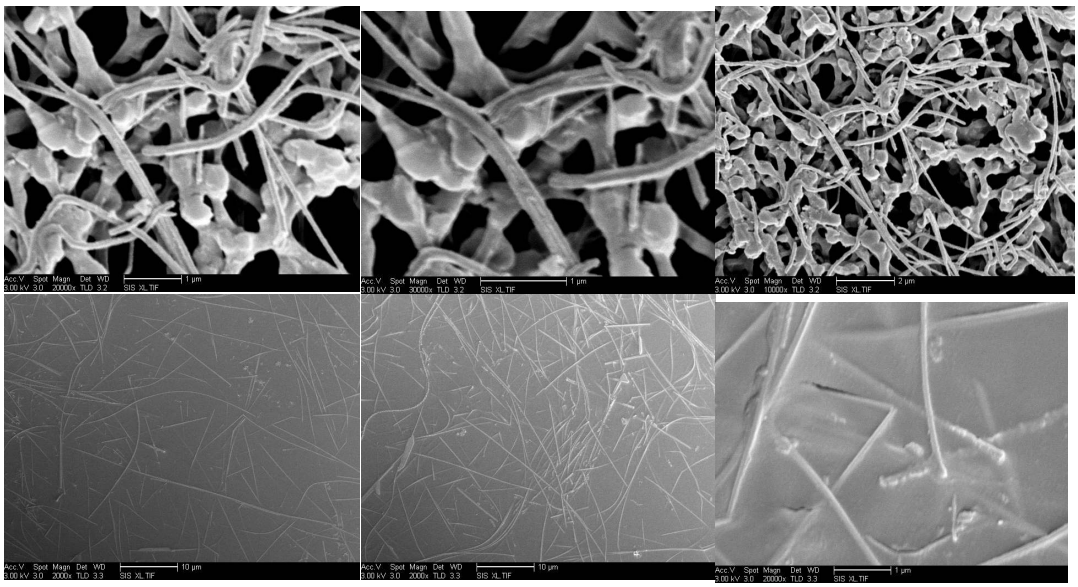

Figure 4.4 SEM of AgNW/NC before (top) and after (bottom) DMSO treatment

To reveal a correlation between morphology and transmittance, we show scanning electron microscopy (SEM) images of each treated nitrocellulose substrate, shown in figure 4.3. The original nitrocellulose substrate has diverse pore sizes, ranging from 100 nm to 1 μm in diameter (Fig. 4.3d) and has the benefit of easily transferring ions to make a large electrical field and set the nanoparticles onto the porous substrate. (Fig. 4.4)

The DMSO treated nitrocellulose substrate has a more uniform morphology (Fig. 4.3a, b and c) than pristine nitrocellulose (R_{rms} value is 466 nm). This nitrocellulose substrate has a low surface roughness of 0.762 nm (R_{rms}) by atomic force microscopy (AFM). However, the roughness of the substrate was increased when the transmittances were reduced: 76% (R_{rms} is 61.5 nm) and the 32.5% (R_{rms} is 159 nm). By the SEM and AFM results, these surfaces roughness has the effect of transmittance; a more uniform surface shows higher transmittances. To control the roughness related with transmittance, mainly it was investigated two factors; the

treatment solvents and temperatures. Figures 4.3a and d show the effect of the solvent and figures 4.3d and g show the effect of temperature during the time when the substrates were made transparent. These substrates which have a controllable diverse range of transmittance can be smeared to allow diverse applications such as touch panels, displays, and solar cells.

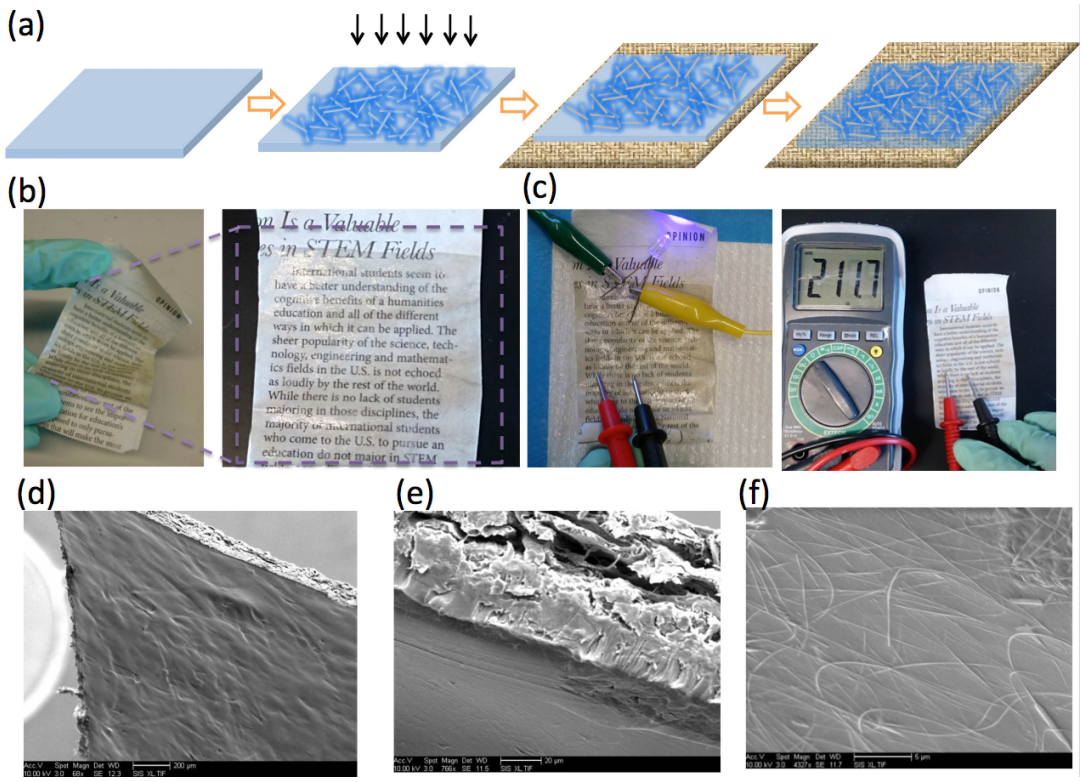

Figure 4.5 Paper electronics (a) process (b) the images of AgNW nitrocellulose film implanted on newspaper (c) the images of test for surface electrical conductivity using LED and multimeter measurement. (d), (e) the vertical SEM images of AgNW nitrocellulose film implanted on newspaper (f) the surface SEM image of the AgNW nitrocellulose film surface.

Figure 4.5a shows the process of AgNW deposition by electrical field and implantation onto a newspaper. First, the AgNW dispersed solution was deposited onto an activated nitrocellulose membrane surface by electrophoretic deposition. A

more detailed process is outlined in the supporting information. After drying, the AgNW deposited nitrocellulose membrane was implanted onto normal newspaper using DMSO. With oven heating at 85 ^{o}C, the nitrocellulose membrane was changed to transparent and implanted onto the newspaper. Figure 4.5d shows SEM images of the implanted newspapers. Even though the surface roughness was increased with the DMSO treated nitrocellulose film fabricated onto a glass surface, the nitrocellulose film was well implanted with the newspaper because the backside of the nitrocellulose membrane had an adhesive material applied to it by the DMSO treatment. The film is ~30μm thick and there is no gap within the contact with the newspaper, shown in figure 4.5e. The AgNWs on nitrocellulose film layered on newspaper formed an electrical network and the sheet resistance value of the surface is 17 Ω/sq (figure 4.5f). More SEM images can be found in the supporting information. Because of the flexibility, adhesion of nitrocellulose substrate, and high transmittance value, the film successfully incorporated paper electronics. This thin film implanted with newspapers and can be bent without shrinking the electrical performance (figures 4.5b and c).

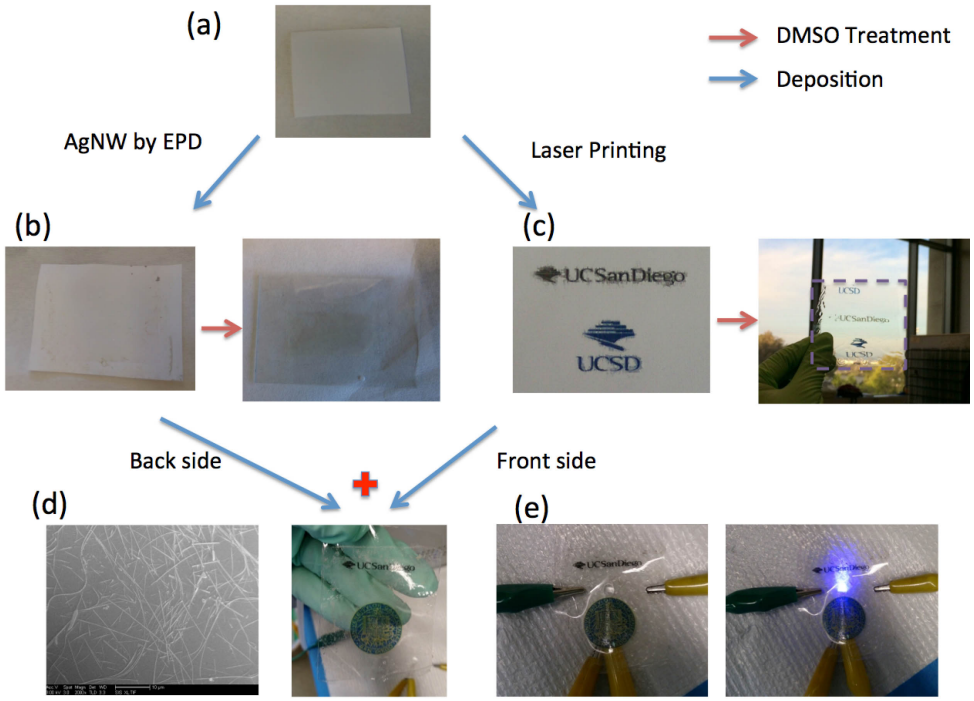

Figure 4.6 Optically transparent and electrically connected AgNW networks on nitrocellulose substrate with pattern (a) a pristine nitrocellulose membrane (b) the images of AgNW networks on nitrocellulose substrate by electrophoretic deposition; before/after transparency (c) the images of laser printed paper-like nitrocellulose substrate; before/after transparency, (d) SEM image of AgNW networks and the transparent nitrocellulose substrate applied by both electrophoretic deposition and laser printing on the top and bottom sides. (e) the demonstration of turning on/off LED diode through the laser printed transparent electrode.

Because this substrate is thin, flexible, porous, and can be applied by various methods, the substrate can be used for diverse applications and methods. First, we demonstrate the printing method on this substrate by a normal office laser printer. The pattern of the UCSD logo was deposited with minimal bleeding due to electrostatics on the surface. After DMSO treatment, however, the pattern of UCSD logo still remained onto the substrate, shown in figure 4.6c. We also demonstrate AgNWs deposition onto this porous substrate by electrical field, shown in figure 4.6b. After drying, the substrate was treated by DMSO to become transparent. The sheet resistance value is

17 Ω/sq. and the nitrocellulose, which smeared into AgNWs networks, was incorporated to act as a binding material, unlike AgNWs freely standing on the substrates. The substrate was melted by DMSO and reconstructed during the drying cycle. During the process, the nanoparticles were implanted inside nitrocellulose substrates, using a superfluous amount of DMSO. This reduced the conductivity of the whole substrate due to breaking or blocking of the nanoparticles network. But the increase in sheet resistance value was very low when the substrate was melted only using a small amount of DMSO.

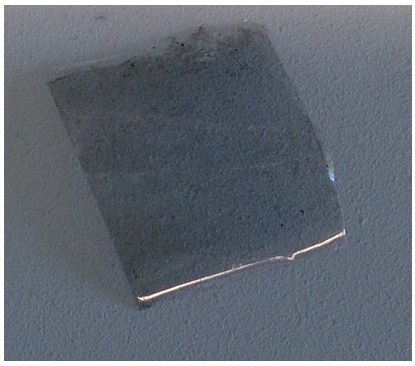

Figure 4.7 Optical image of CNT deposition by spray method (after DMSO treatment)

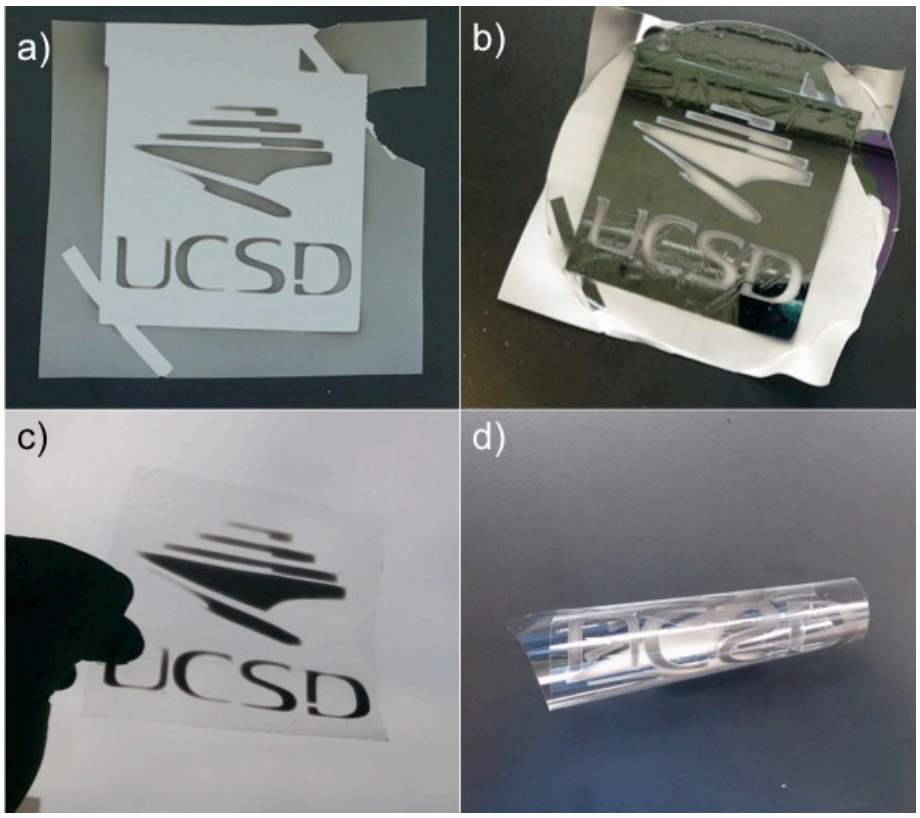

Figure 4.8 Optical image of Ti/Al deposition by metal sputtering method (before/after DMSO treatment)

One of the major strengths of using this substrate is the ability to apply different methods on each side of the substrate. We demonstrate that the substrate was fabricated onto one side by electrophoretic deposition and on the other side by laser printing. After that, the substrate was treated with DMSO and became transparent, shown in figure 4.6d. The film has the AgNW network on the nitrocellulose surface and a sheet resistance value of 17 Ω/sq. Optically transparent substrate patterned with the UCSD logo successfully turned an LED on and off through this substrate (figure 4.6e). In another approach, we demonstrate the spraying method, shown in figure 4.7, and aluminum sputtering method, shown in figure 4.8. However, we expect that this nitrocellulose membrane can not only be used with the methods investigated in this

paper, but this unique substrate can also be applied to silk-screen for bio-sensor, paper printed microfluidics, roll to roll for organic solar cells and inkjet print electrodes. In this paper, we also show the nitrocellulose film implanted on cloth.

4.4 Conclusion

In conclusion, this unique nitrocellulose substrate can be applied to diverse methods for multidisciplinary use. Here, we have shown that the nitrocellulose substrates have controllable transmittance by different solvent treatments and conditions. This substrate was functionalized by deposition under a variety of methods: laser printing, AgNW deposition by electrophoretic deposition, aluminum deposition by shadow masking, and spraying. The transparent process for the nitrocellulose substrate has benefits for use with double sides for deposition and the ability to be implanted onto other materials such as newspaper and garments since the nitrocellulose functions as a glue. Since this flexible film has a high transmittance without losing electrical properties, the film can be used for diverse application such as touch screens, solar cells, and organic light emitted diodes. Also, the biocompatibility of nitrocellulose is high due to its extraction from woods.

Chapter 4, in part, has been submitted for publication of the material as it may appear in Advanced Materials: Youngjun Song, Yvonne Heaney, Tsukasa Takahasi, Sejung Kim and Michael J. Heller, Flexible, Transparent, and Implantable Nitrocellulose Substrates for Electronic Devices. The dissertation author was the primary investigator and author of this paper.

Chapter 5: A Programmable DNA Double Write Material – Synergy of DNA Photolithography and Self-Assembly Nanofabrication

5.1 Introduction

Functional biomaterials based on DNA allow both patterning, which has been developed in a variety of methods and applications, and nanostructure self-assembly, which can be functionalized with nanoparticles through the base sequence information in the DNA strand. The primary key fact to allow for these functionalities is that DNA oligonucleotide sequences with just 40 bases (1.25nm x 13.6nm in size) can provide a huge number of highly specific programmable nanoscale linkers each with a unique binding identity. Self-assembly by hybridization of complementary DNA sequences derivatized with fluorophores, nanoparticles and other entities is a rapid, simple and selectively desired binding process compared to other methods that utilize chemical binding agents.

Conventionally, DNA strand patterns were performed for top-down photolithography with pre-patterning using polymer-blocking materials such as polymethyl methacrylate (PMMA) by electron beam lithography and UV lithography with a singular ID. New approaches for patterned DNA and DNA nanoparticles were investigated by a range of techniques to create merged top-down and bottom-up methods including micro-contact printing, free standing silk screen patterning, free stranding onto nanosize pre-patterned etched template substrate and AFM tip. However, these researches showed weaker binding energy such as electrostatic binding and free standing, and were time consuming in comparison to conventional

methods.

In an aim for DNA patterning by UV lithography, which can be fabricated quickly and easily to make mass products, the UV sensitive chemical cross-linkers were studied with programmable binding of DNA information. In 2003, the author (Heller et al.) invented the UV lithographic technique for DNA patterning a substrate using psoralen conjugated nucleotides to produce cross-linking between two DNA strands22, and studied the patterning of DNA through whole gene information knockout by a long time, deep UV exposure (2 hours). Recently, Lang Feng et al. also demonstrated conjugated DNA sequences using the artificial UV cross-linker base cinnamate to produce inter-strand cross-linking. Without controlling the property of DNA binding which allows for informational self-assembly by Watson-Crick base paring, these DNA patterning researches were assisted by UV reacted chemical bonds such as psoralen and cinnamate which are sensitively active on 360nm wavelength to immobilize DNA strands.

Here, unlike the chemical DNA immobilization processes and the whole gene knockout process, we have designed the selective controlling DNA hybridization focusing on the fact that thymine bases are sensitive to deep UV to block the DNA information and the short base pairs displacement reaction effect. This information controlling was made possible by a short time, deep UV exposure for the thymine dimer, investigated to estimate an appropriate amount for a UV dose. The sequence that we designed is based on indiscrete thymine bases allowing in the DNA double write for the DNA strand to selectively bind via the displacer effect where partially

pre-hybridized DNA can block or replace secondary DNA probes. Also, we show diverse benefits with high resolution, multilayer patterns of biomaterials in the DNA double write sequence and process.

We believe deep UV photolithographic based methods for DNA patterning have important advantages which include: (1) integrates well with established semiconductor manufacturing processes which have been developed for 20nm patterning size; (2) has a high potential for uniformity and consistency; and (3) can produce heterogeneous layered 3D structures; (4) has selective self assembly controlled by deep UV; (5) allows arrays to detect sensitive reporter group-fluorescently labeled short probes.

5.2 Methods

5.2.1 List of DNA sequences

All of the designed sequences were ordered from Integrated DNA Technologies, Inc.

- The gel experiment DNA sets are:

5’-TTT TTT TTT TTT TTT TTT TTT TTT-3’

5’-Cy3-AAA AAA AAA AAA AAA AAA AAA AAA-3’

5’-FAM-AAA AAA AAA AAA AAA AAA AAA AAA-3’

5’-AAA AAA AAA AAA AAA AAA AAA AAA-3’

5’- Cy3-TTT TTT TTT TTT TTT TTT TTT TTT-3’

5’-TTT TTT TTT TTT TTT TTT TTT TTT CCC GCC CGC CCG CCC G-3’

5’- FAM -GGG CGG GAA AAA AAA AA-3’

5’- FAM -GGG CGG GCG GGC GGG C-3’

- The substrate pattern experiment DNA sets are:

NH_2-C6-5’-TTT TTT TTT TTT TTT TTT TTT TTT CCC GCC CGC CCG CCC G-3’

5’-TTT TTT TTT TTT TTT TTT TTT TTT GGG CGG GCG GGC GGG C-3’

5’-Alex546-GGG CGG GAA AAA AAA AA-3’

5’-Alex488-GGG CGG GCG GGC GGG C-3’

5’-Alex546-AAA AAA AAA AAA AAA AAA AAA AAA-3’

5’-Alex488-AAA AAA AAA AAA AAA AAA AAA AAA-3’

5’- biotin-AAA AAA AAA AAA AAA AAA AAA AAA-3’

5’-AAA AAA AAA AAA AAA AAA AAA AAA CAG GAC AGA CAG G -3’

5’-Alex647-CCT GTC TGT CCT G -3’

5.2.2 Preparation of DNA sequences

All of the designed sequences were ordered from Integrated DNA Technologies, Inc. The sequence of immobilized ssDNA, WS:ID1&ID2 on the substrate was NH_2-C6-5’-TTT TTT TTT TTT TTT TTT TTT TTT CCC GCC CGC CCG CCC G-3’. The sequences used for the double write (SWP,DWP) were 5’-Alex546 (ex555nm, em571nm)-GGG CGG GAA AAA AAA AA-3’ and 5’-Alex488 (ex492nm, em517nm)-GGG CGG GCG GGC GGG C-3’. For the double write with second level write, the first red fluorescent complementary probe sequence for the single level write probe was 5’-Alex546 (ex555nm, em571nm)-AAA AAA AAA AAA AAA AAA AAA AAA-3’. The ES:ID2’&ID1 sequence was 5’-TTT TTT TTT TTT TTT TTT TTT TTT GGG CGG GCG GGC GGG C-3’. The sequence of the second green

fluorescent complementary probe was 5'-Alex488 (ex492nm, em517nm)-AAA AAA AAA AAA AAA AAA AAA AAA-3'. The sequence used for the biotinylated probe was 5'- biotin-AAA AAA AAA AAA AAA AAA AAA AAA-3'. The sequence for the short base pairs target sequence was 5'-AAA AAA AAA AAA AAA AAA AAA AAA CAG GAC AGA CAG G -3'. The sequence for the far red fluorescent complementary probe to detect target sequence was 5'-Alex647 (ex650nm, em670nm)-CCT GTC TGT CCT G -3'.

5.2.3 Polyacrylamide gel analysis

The lane 1 sample was prepared with 10µl Cy3-A_{24} (20µM) mixed with 5µl T_{24} (20µM) without UV light exposure and left for 10 minutes before running with ssDNA and dsDNA ladders. The lane 2 sample was prepared with 5µl UV exposed A_{24} (20µM) mixed with 5µl Cy3-T_{24} (20µM) and left for 10 minutes to hybridize. The lane 3 sample contained 5µl Cy3-A_{24} (20µM) with 5µl UV-exposed T_{24} (20µM) and left for 10 minutes to hybridize. The UV exposed conditions were 254nm wavelength for a period of 7 minutes. The 20% polyacrylamide gel in 0.5 X TBE buffer was run at 200V for 60 minutes. Also, after the samples were prepared 10ul volume of 10µM, other gels were run with a same condition were run at 160V for 120 minutes.

5.2.4 Preparing the ssDNA strand for immobilization onto the substrate

Covalently bonded ssDNA functional glass slides were prepared in two steps using amine (NH_2) activated glass slides (Thermo Fisher Scientific, Inc.). First, 100mM of disuccinimidyl suberate (DSS), a homofunctional NH_2-to- NH_2 crosslinker, was dispersed in dimethyl sulfoxide (DMSO) and applied to the NH_2-activated glass

slide. The mixture was reacted for 1 hour at room temperature. Then the glass slides were washed twice with DMSO and DI water, and dried with Nitrogen (N_2) gas. 20μM NH_2-ssDNA strands (NH_2-C6-5'-TTT TTT TTT TTT TTT TTT TTT TTT CCC GCC CGC CCG CCC G-3') in 1X SSC buffer were applied and reacted for 1 hour at room temperature. The glass slides were again washed twice with 1X SSC buffer and dried with N_2 gas.

5.2.5 Patterning by UV lithography

The power of a 254nm/302nm/365nm UVC hand lamp (UVP, LLC) was measured at a working distance of 2cm with a 254nm/302nm/365nm peak photodiode (Newport Corporation). The 254nm UV wavelength power was calculated to be 3mW/cm^2. Also, others wavelengths were measured similar power with 254nm. The photomask was designed down to 500nm resolution in AutoCAD (Autodesk, Inc.) and then purchased from Phototronics, Inc. The substrate bonded with ssDNA was vacuum-contacted with a custom-designed chrome photomask and aligned using the MA-6 mask aligner. UV light was exposed on the substrate through the photomask for 5 minutes.

5.2.6 Double write hybridization

After the ssDNA-immobilized substrate was patterned by UV exposure, 20μl of the first writing solution (20μM), 5'-Alex546 (ex 555nm, em 571nm)-GGG CGG GAA AAA AAA AA-3' in 1X SSC, was placed on the substrate and covered with a cover slip. After hybridizing the substrate for 1 hour at room temperature, the substrate was washed with 1X SSC buffer using a 250ml water bath at room temperature for 1 minute. After this washing step was repeated the substrates were dried with N_2 gas. To

complete the double write, 20µl of the second writing solution (20µM), 5'-Alex488 (ex492nm, em517nm)-GGG CGG GCG GGC GGG C-3', was placed on the substrate and covered with a cover slip. After hybridizing the substrate for 1 hour at room temperature, the double write substrates were washed twice with the 1X SSC buffer and dried with N_2 gas. After hybridization and washing, the substrate was imaged by confocal microscopy (Olympus FV1000). All images were processed by Image J (NIH, Bethesda, MD).

5.2.7 Double write with second level write hybridization

After the WS:ID1&ID2, conjugated substrate was patterned by UV exposure, 20µl of 20µM of the first level writing red fluorescent complementary probe (Alex546-A_{24}) in 1X SSC was left to hybridize on the substrate for 1 hour at room temperature. Then the substrate was washed twice with 1X SSC buffer and dried with N_2 gas. This process was repeated under the same conditions for the ES:ID2&ID1 solution. After that, the substrate hybridized with ES:ID2'&ID1 for the double write with second level write was aligned using pre-marked cross-lines. UV light was exposed for 5 minutes on the substrate, which was vacuum-contacted to the photomask. 20µl of 20µM of the second level writing green fluorescent complementary probe (Alex488-A_{24}) in 1X SSC was left to hybridize on the substrate for 1 hour at room temperature. Then the substrate was washed twice with 1X SSC buffer and dried with N_2 gas. The substrate-patterned double write with second level write was monitored by confocal microscopy (Olympus FV1000).

5.2.8 Target sequence double write with second level write hybridization

After the first level write and hybridization by the red fluorescent complementary probe (Alex546-A_{24}), the ES:ID2'&ID1 hybridization process was repeated under the same conditions as the double write with second level write hybridization. After UV exposure and alignment, 20µl of 20µM of target sequence probe in 1X SSC was left to hybridize on the substrate for 1 hour at room temperature. Then the substrate was washed twice with 1X SSC buffer and dried with N_2 gas. After that, 20µl of 20µM of the far red fluorescent complementary probe (5'-Alex647-CCT GTC TGT CCT G -3') in 1X SSC used to detect target sequence was left to hybridize on the substrate for 1 hour at room temperature. Then the substrate was washed twice with 1X SSC buffer and dried with N_2 gas. The substrate-patterned target sequence double write with second level write was monitored by confocal microscopy (Olympus FV1000).

5.2.9 Protein double write with second level write hybridization

After the WS:ID1&ID2 conjugated substrate was patterned by UV exposure, 20µl of 20µM of the first level writing green fluorescent complementary probe (Alex488-A_{24}) in 1X SSC was left to hybridize on the substrate for 1 hour at room temperature. Then the substrate was washed twice with 1X SSC buffer and dried with N_2 gas. This process was repeated under the same conditions for the ES:ID2'&ID1 solution. Then, the substrate hybridized with ES:ID2'&ID1 for the double write with second level write was aligned using pre-marked cross-lines. UV light was exposed for 5 minutes on the substrate, which was vacuum-contacted to the photomask. The

biotinylated probe (Biotin-A_{24}) in 1X SSC was left to hybridize on the substrate for 1 hour at room temperature. Then the substrate was washed twice with 1X SSC buffer and dried with N_2 gas. Cy3-Streptavidin (Sigma-Aldrich, Inc.) was attached on a patterned biotinylated probe hybridized substrate and washed twice with 1X PBS. After, the substrate was dried with N_2 gas, and the substrate-patterned SSP double write with second level write was monitored by confocal microscopy (Olympus FV1000).

5.3 Results and Discussion

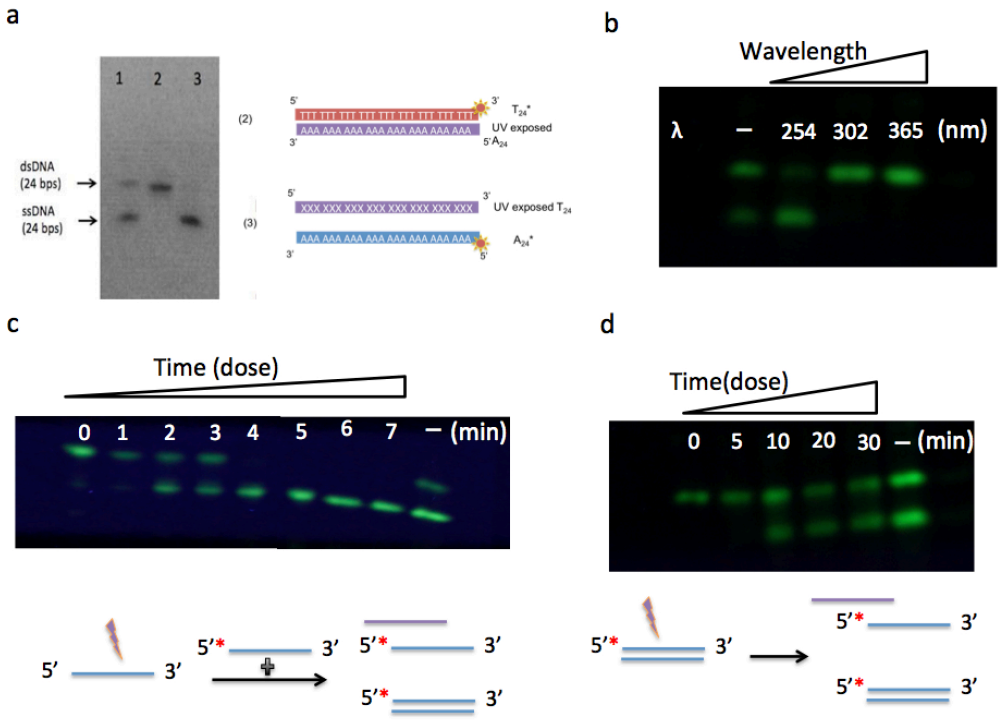

Figure 5.1 The polyacrylamide gels for thymine dimer. a, blocking hybridzation of the thymine dimer, lane 2 ($A_{24}|T_{24}$*), lane 3 ($T_{24}|A_{24}$*). **b, c,** the binding after UV exposed ssDNA (T_{24}) by wavelength (b) and time (c). **d,** dehybridization of dsDNA ($T_{24}|A_{24}$*) by thymine dimer.

The mechanism for blocking DNA hybridization is the thymine dimerization of

ssDNA induced by deep UV. Exposure of DNA containing thymine bases to short wavelength UV light (~254nm) causes thymine dimer formation (via cyclobutane thymine dimers, 6-4 photoproduct). The dimerization of the thymine bases prevents hydrogen bonding to the adenine bases in the complementary DNA sequence. Initially, to understand the concept of the thymine dimerization, we show an electrophoretic (PAGE gel) separation demonstrating that a UV exposed A_{24} oligonucleotide still hybridizes to a complementary Cy3-T_{24} oligonucleotide (lane 2), while a fluorescent Cy3-A_{24} oligonucleotide does not hybridize to a UV exposed T_{24} oligonucleotide (lane 3), shown in figure 5.1a. To show and optimize patterning applications using thymine dimers, we developed an assay using T_{24}, which we primarily use in our system. In Figure 5.1b, different UV wavelengths (254nm, 302nm, 365nm) were exposed to T_{24} for 5 minutes to configure a design for short time irradiation. Only 254nm was found to effectively allow for hybridization blocking. Next, we investigated the amount-dose effect. In Figure 5.1c, T_{24} blocking for hybridization was examined under varying exposure times to determine the dosage amount of constant deep UV power to be 3 mW/cm^2 at 2 cm working distance. A 2 minutes exposure was not enough to completely block hybridization, however, after 5 minutes, the thymine dimerization was enough to block hybridization of complementary DNA (A_{24}*). In another set of thymine dimer experiments, we investigated the time in which dsDNA ($T_{24}|A_{24}$*) changed to ssDNA (T_{24} and A_{24}*) by deep UV thymine dimerization, shown in Figure 5.1d. The time was investigated at intervals up to 30 minutes. For a 5 minutes exposure, dsDNA ($T_{24}|A_{24}$*) strongly bound with complementary DNA, but dsDNA started to lose its hybridization bond starting at 10 minutes exposure time without

DNA single-strand breaks[31] (Figure 5.1d, last lane on the right). Thus, these results allow the creation of DNA sequence designs for informational patterning for short time deep UV exposure as well as a secondary exposure within the 10 minutes after first hybridization.

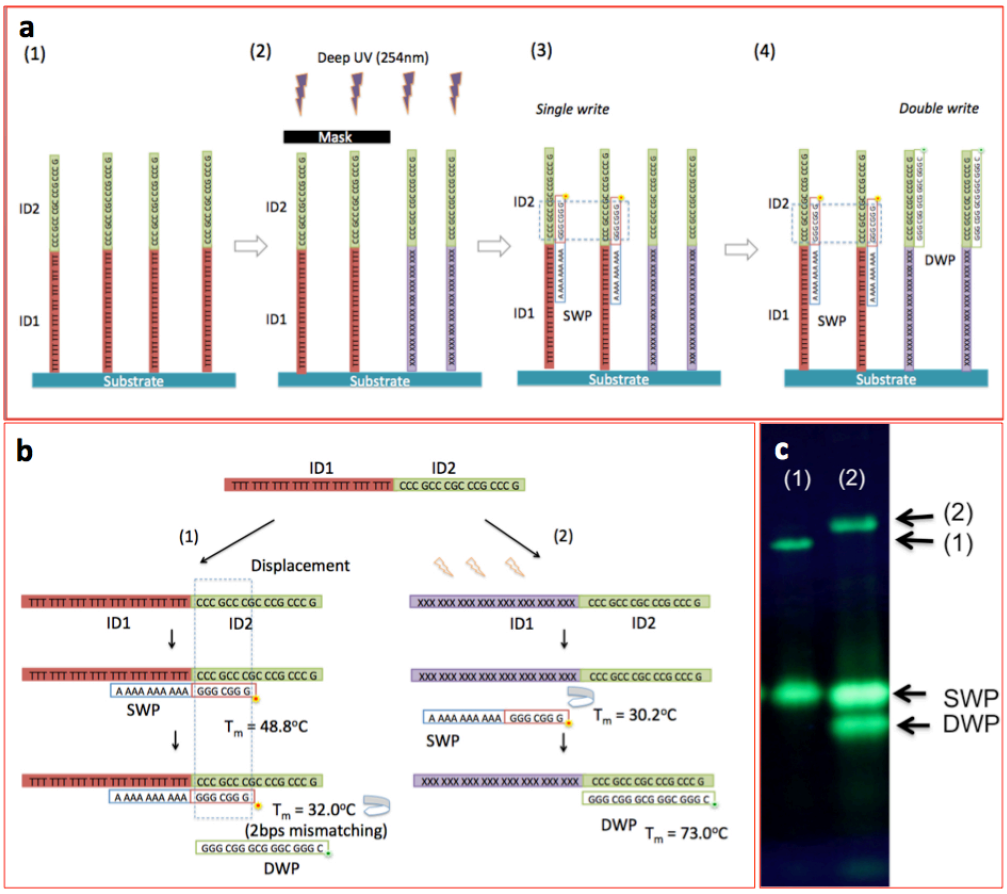

Figure 5.2 Scheme of *DNA double write* by UV photolithography and displacer effect. a, the process of *DNA double write.* **b,** displacer effect by thymine dimer and the melting temperatures of sequences. **c,** the results of 20% polyacrylamide gel electrophoresis for displacer effect by thymine dimer.

Table 5.1 *DNA double write* sequence melting temperature and binding energy. SW:ID1&ID2|SWP* (2-3 mismatching due to alex 546 molecular (*)).

DNA		Binding Energy			UV
Probe	Template	Tm (°C)	bps	Hybridization	Action
SWP*	WS:ID1&ID2	48.8	17	High	Write (1)
SWP*	WS:ID2	30.2	7	Low	Block
DWP*	WS:ID2	73	16	High	Write (2)
DWP*	WS:ID1&ID2|SWP*	21.4-32	7-8	Low	Block

The sequences and process for carrying out the *DNA double write* photolithography and initial write results are shown in Fig. 5.2 and Fig. 5.3. The *DNA double write* performed geometrical patterning with two IDs through the physical and thermodynamic changing of the sequence information.

The unique sequence for the *DNA double write* was designed to allow two distinguishable identities to bind by deep UV photolithography, based on the quantitative results for the hybridization and blocking of DNA in Figure 5.1. The sequence for the *DNA double write* is 5'-TTT TTT TTT TTT TTT TTT TTT TTT (ID1)-CCC GCC CGC CCG CCC G (ID2)-3'(fig. 5.2a, b). This specially designed DNA write sequence (WS:ID1&ID2) has two sections, ID1 (red, fig 5.2a, b) and ID2 (green, fig 5.2a, b), which after UV exposure allow the two different complementary probes to be separately hybridized to the unexposed regions (red, fig.5.2 a and b (1)) and the UV exposed regions (purple, fig. 5.2a and b (2)) respectively. Two different complementary probes were designed, with the sequence of the red fluorescent complementary probe for the single writing probe (SWP) as 3'-AAA AAA AAA AGG GCG GG-Alex546-5' and the sequence of the green fluorescent complementary probe for the double writing probe (DWP) as 3'-GGG CGG GCG GGC GGG C-Alex488-5'. All lists of sequences and binding diagram are in Methods and Supporting Information.

The design of UV inactivation of the thymine bases in the ID 1 (red) area of the WS:ID1&ID2 sequence is of key importance for the double write process. However, the design of the ID2 (green) sequence and the design of the SWP and DWP sequences

were considered with regards to the melting temperatures of the whole sequences, which were considered with/without the expectation of thymine blocking. Because of these binding energies that are calculated based on the melting temperature, the SWP and DWP can be selectively bonded onto WS:ID1&ID2 or deep UV exposed to WS:ID2 (ID1 is inactivated by deep UV, purple at fig 5.2b) by short base pairs (bps) displacer effect. First, WS:ID1&ID2 only allow binding to the SWP, while WS:ID2 could not allow binding to the SWP due to binding energy, which is 30.2^{o}C for 5'-CCC GCC C-3'. As the DWP sequence can hybridize to the ID2 (green) sequence in both the UV exposed and un-exposed areas, the SWP must be designed to prevent hybridization of the DWP in the un-exposed areas. (Fig. 5.2b (2), Table 5.1) This is accomplished by designing the SWP probe so it is not only complementary to the ID1 (red in fig. 5.2b) sequence of the WS:ID1&ID2, but also has a short segment of sequence (GGG CGG G) that overlap with a section of the ID2 (green in fig. 5.2b) sequence. The partially hybridized DNA (WS:ID1&ID2|SWP* at Table 1) could not allow binding to DWP due to short bps sequence displacement, which makes blocking (T_m= 21.4-32^{o}C) another probe on the DNA template with 2-3 mismatched bases because of alex 546 molecular. (Fig. 5.2b (1), Table 5.1)

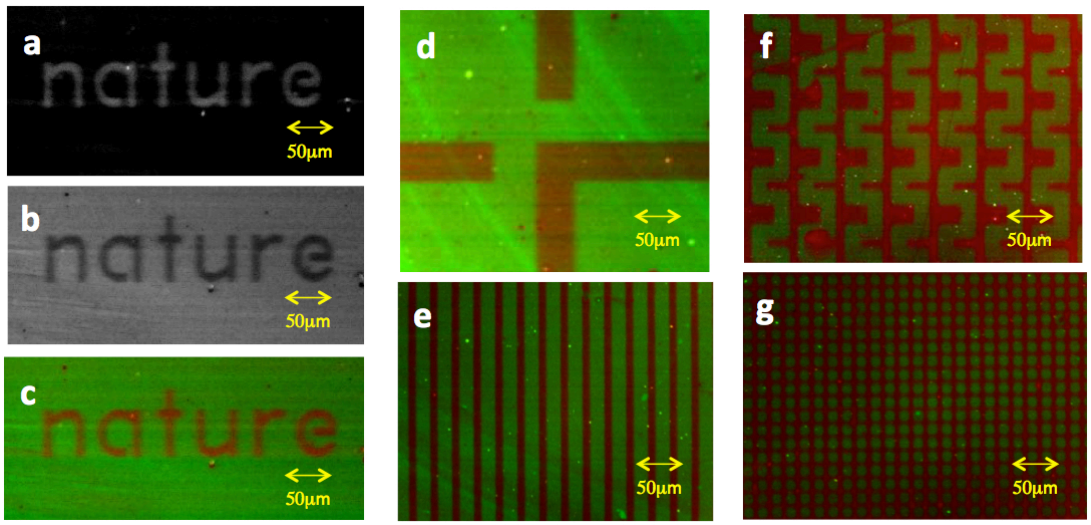

Figure 5.3 Confocal images of *DNA double write* by UV photolithography. a, image of the single write; FWP was hybridized on the letters. **b,** image of the second write; SWP was hybridized without letters. **c,** the *double write* image which was merged from single write (a; red color) and second write (b; green color). **d-g,** more *double write* images (first write color is red, second write is green).

In fig 5.2 a, the first step in the process is the immobilization of the specially designed *DNA double writing* sequence onto the glass substrate surface. The second step (Fig. 5.2a (2)) in the process is photomasking and UV light exposure, which is carried out for 5 minutes. The third and fourth steps (Fig. 5.2a (3), (4)) are hybridization of the red SWP probe sequence and the green fluorescent DWP sequence, respectively. Generally these hybridization steps take about 30 minutes including the wash steps. Figure 5.3 shows results for the DNA double write using the immobilized WS and the red fluorescent complementary probe and green fluorescent complementary probe. The letters in the patterned feature (nature) are approximately 40µm in width, resulting from the hybridization of the red fluorescent complementary probe in the un-exposed areas. Figure 5.3a shows a black and white fluorescent image of the hybridized red SWP (ex555nm, em571nm) as white letters on a black

background. Figure 5.3b image shows the hybridized green DWP (ex492nm, em517nm) as a white background with darker letters. Figure 5.3c shows the false color image with the red fluorescent letters (nature) and the green fluorescent background. Finally, figure 5.3d-g shows a variety of other UV patterned images using the *DNA double write* photolithographic process. Some of the spotting and blemishes are due to imperfections and inhomogeneity on the substrate surface. If necessary, the hybridization step can be carried out under slightly higher stringency (higher T_m) to improve the specificity of the SWP and DWP probes to un-exposed and UV exposed areas respectively.

This ability to produce two distinguishable identities for hybridizing by deep UV irradiation and the displacer effect is an important and unique attribute of the *DNA double write* process. We believe that this attribute extensively impacts DNA nanotechnology, as a new method to rapidly and easily control DNA. For example, DNA origami, which is self-assembled in a variety of forms, can manipulate its appearance using a UV exposure trigger. Also, this may affect the DNA chemical computing system using this displacer effect on the ssDNA with a higher melting temperature and the concept of surface connected DNA computing which is cleaved by an enzyme to build an enzyme-free system which allows the translation system for the sequence-specificity.

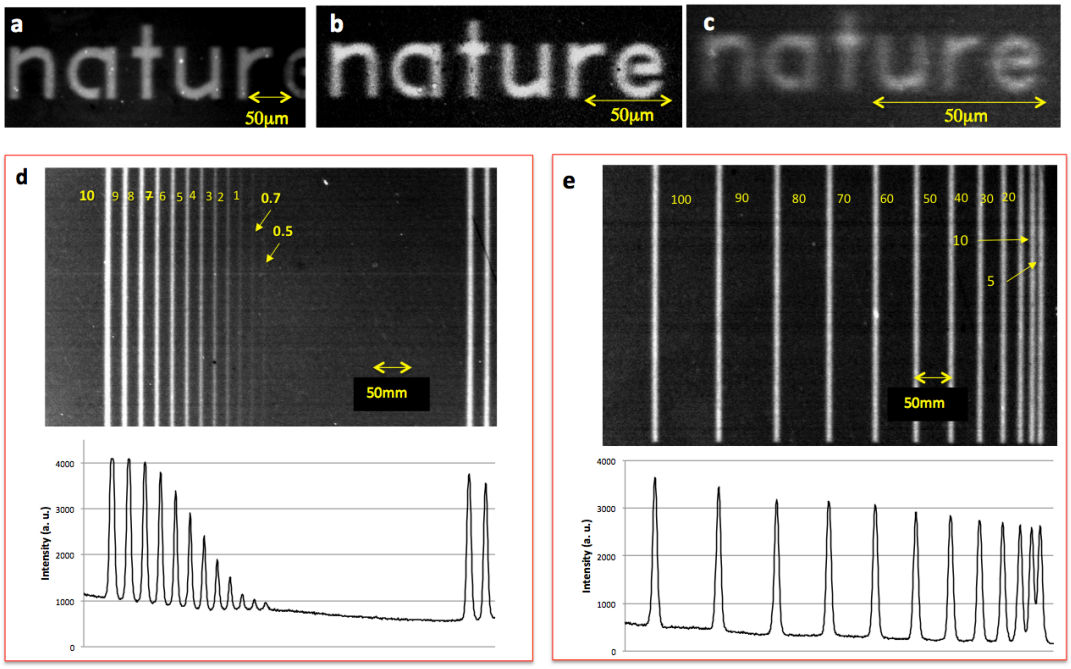

Figure 5.4 ***DNA double write*** **with first level write. a, b, c,** the images of letters (10μm line, 5 μm line, 2 μm line). **d,** the lines resolution from 10μm to 500nm. **e,** the gap resolution from 100μm to 5μm.

To better recognize DNA patterns through deep UV exposure, the first set of experimental results were obtained from the double write sequence on the substrate, which has a thin DNA layer (1.2nm-13.6nm) for high resolution processing[40]. In the first step, the DNA writing sequence (WS:ID1&ID2) was immobilized on the glass substrate surface. After exposure to deep UV light (254nm) for 5min through the photomask onto WS:ID1&ID2 immobilized on the substrate, a red fluorescent complementary probe (A_{24}*) was hybridized onto the substrate. Figure5.3b-h shows three sets of images for the patterned feature, where line widths for the letters are 10μm (Fig. 5.4a), 5μm (Fig. 5.4b) and 2μm (Fig. 5.4c). The line edge of the letters is very clear. Figure 3d and e provide further results for patterned line images, which show line widths from 10μm down to 500nm, with 20μm spacing gaps (Fig. 5.4d) and

patterned spacing gaps from 100μm to 5μm with 10μm line width (Fig. 5.4e). Also, in the Supporting Information, we show the same experiment using WS:ID1&ID2 electrostatically bound on the amine glass slide. The pattern contained more blemishes, but the probe was hybridized with the informational pattern with high resolution (500nm) lines. Again, we believe that some of the distortion and blemishes are due to inhomogeneity of the substrate surface itself and it can be controlled by washing conditions or using a homogeneous substrate.

This result shows three times higher resolution (Figure 5.4d) compared with photo-crosslinking chemistry DNA pattern reports. There are two main reasons to achieve such high resolution (500 nm) in vacuum photolithography; (1) using a deep UV system (32nm resolution for 254nm KrF light source, 21nm resolution for 192nm ArF light source) and (2) having an ultrathin layer (1.2nm-13.6nm), which has a critical effect on the obtainable high resolution. Also, this direct DNA write technique combined with top-down and bottom-up methods allows for the reduction of contaminants due to no additional processing steps, and in consequence, effectively minimizes the chance of defects in the resulting structures. Following the scale rule (Moore's Law) in semiconductor manufacturing, we expect much better feature resolution and shorter (within a few seconds) UV exposure with higher performance photomasking and an x-y-z positioning projection system, such as a stepper which supplies high energy, deep UV (192nm, 254nm) irradiation.

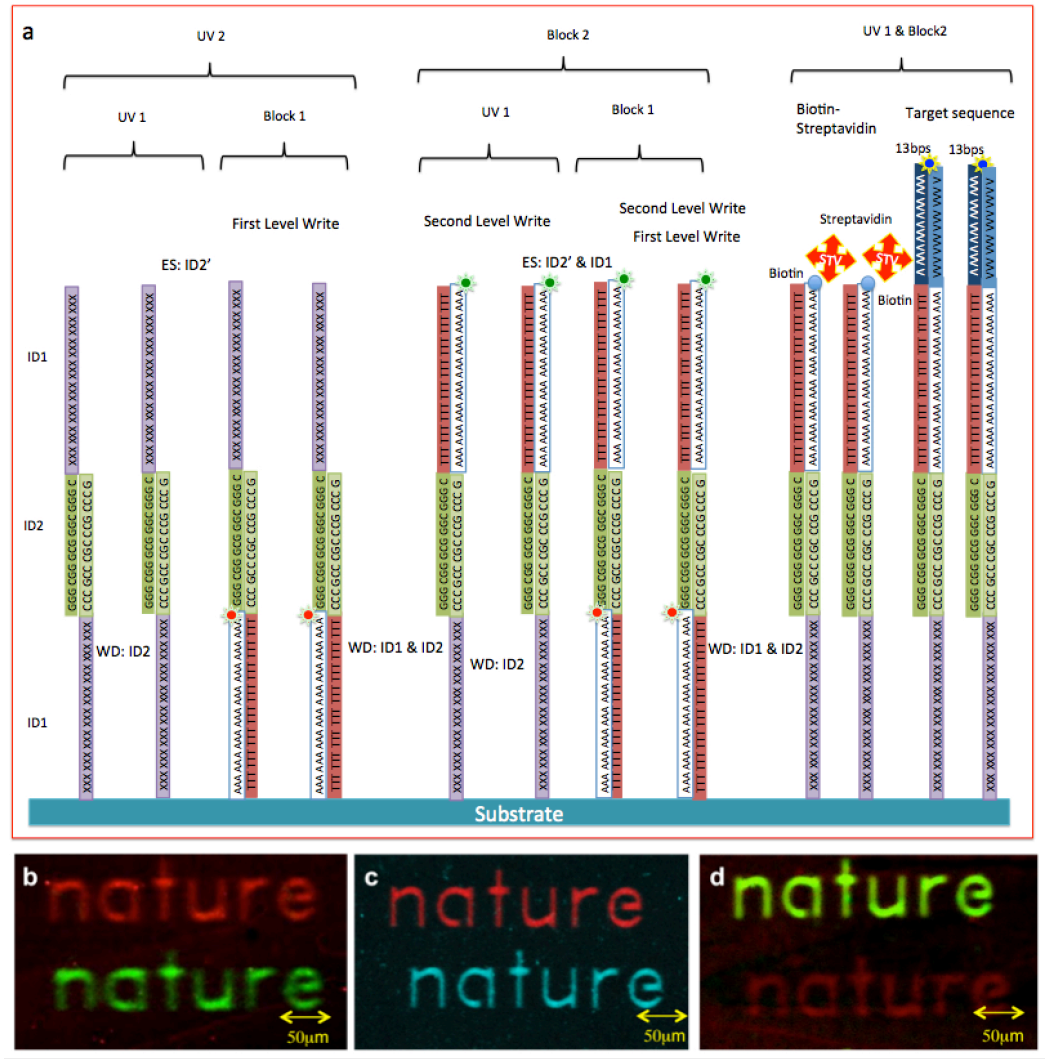

Figure 5.5 Scheme and results of *DNA double write* with second level write including the detections of target sequence and protein. a, the representation of second level write sequence and probe **b,** the confocal image of the *DNA double write* with a second level write **c,** the confocal image of the *DNA double write* with a second level write for pattern detection of target 13 bps DNA sequence **d,** the confocal image of the DNA double writing with a second level write for pattern detection of streptavidin

To pattern multiple layers and diverse biomolecules in addition to a first level write, we have also demonstrated a second level write using extended layered DNA, which is hybridized at section ID2 in WS:ID1&ID2. The extended layered sequence (ES:ID2'&ID1) is 3'- CGG GCG GGC GGG CGG G(ID2')- TTT TTT TTT TTT TTT

TTT TTT TTT(ID1)-5'. The ID2' section of ES:ID2'&ID1 is hybridized to the ID2 section of the first level write sequence (WS:ID1&ID2). A second photomasking step is carried out and then a second level probe sequence can be hybridized to the UV exposed and/or the un-exposed second level areas by a green fluorescent complementary probe. The red fluorescent complementary probe of the first level write is hybridized to the ID1 segment of the WS:ID1&ID2 sequence and the green fluorescent complementary probe of the second level write is hybridized to the ID1 segment of the ES:ID2'&ID1 sequence. The false colors fluorescent image of the first and second level writes is presented by red and green. The DNA sequence information for the second level write and the hybridization is represented in figure 5.5a and results are shown in figure 5.5b. Because the dimerization time for the hybridized thymine bases (dsDNA) was twice as long as the ssDNA's thymines in figure 1 d, this allows for a second level write (green letters in figure 5.5b). The advantage of this DNA second level process is that it can perform layering of patterns. To show more results, the double level write was overlapped on the nature letter (single level write), in Supporting Information. This is important as it shows that the process allows second level UV patterning as well as further hybridization based self-assembly to be carried out.

For pattern detection of a 13 bps target DNA sequence (5'-CCT GTC TGT CCT G-3'), the process for the second level write for the specific sequence DNA is represented to the rightmost side of figure 5.5a and pattern detection is successfully demonstrated in figure 5.5c. The false colors fluorescent image of the first and second level write where the red fluorescent complementary probe is hybridized to the ID1

and a far-red fluorescent complementary probe is hybridized to the target designed segment (3'-A_{24}-CCT GTC TGT CCT G-5') were presented by red and blue. In other cases for pattern detection protein, the second level write sequence hybridized was a biotinylated probe (Biotin-A_{24}). After secondary hybridization, the probe was labeled with fluorescent Cy3 streptavidin (Figure 5.5d; first level write is green and second level write with streptavidin is red). This is of further importance as it demonstrates that in addition to self-assembly by hybridization, it is also possible to use biotin-streptavidin ligand binding for further self-assembly.

5.4 Conclusion

In this thesis, we show selective DNA information changing by the deep UV photolithography technique. The *DNA double write* process allows for two distinguishable ID probes to be hybridized in both the UV exposed and non-exposed areas with geometrical patterning by displacer effect. The DNA thymine dimer of the *DNA double write* sequence was carried out to pattern at 500nm high resolution. Using the *DNA double write sequences*, we show the multiple layered DNA hybridization with appropriate patterns. Furthermore, this process is performed with the target sequence and biotin streptavidin binding reactions. This may be performed at higher resolutions and shorter times by a stepper, which can be used for high energy deep UV (192nm, 254nm) and diverse detections of DNA/RNA/PNA sequences and secondary protein bindings. Most importantly, these designs do not preclude encoding large numbers of unique binding identities into the DNA sequences. The approaches of the displacer effect, two distinguishable identities after UV exposure which allows for two different complementary probes, can create a new methodology around the novel top-

down photolithographic applications of DNA including optical DNA memory, DNA nanoparticle self-assembly, DNA microarray sequence chip technology and even DNA substrate computing without enzymes. Also, since we monitored solution based DNA thymine dimer reactions including a unique sequence with other base pairs, there have been great expectations regarding novel bottom-up self-assembly applications of DNA including 3D DNA origami self-assembly triggered by UV, movement of DNA such as DNA motor and DNA walker, DNA nanoparticle self-assembly and DNA chemical computing. The most significant benefit of the *DNA double write* system is that it's easy to be combined with other techniques for diverse purposes based on the selective DNA binding energy change, since intrinsic DNA sequence information can be controlled without DNA modification through UV light irradiation. The *DNA double write* process we have described meritoriously represents the merged technology of top-down and bottom-up processes, due to DNA information control binding that other chemical binders could not show. This technology may have true synergistic effects on multidisciplinary research fields including biotech, material science, computer science and biology of the future what we described the related researches.

Chapter 5, in part, has been submitted for publication of the material as it may appear in Nature Materials: Youngjun Song, Tsukasa Takahashi, Sejung Kim, Yvonne Heaney, John Warner, Shaochen Chen, Michael J. Heller, A Programmable DNA Double Write Material – Synergy of DNA Photolithography and Self-Assembly Nanofabrication. The dissertation author was the primary investigator and author of this paper.

Chapter 6: Conclusion and Future Works

6.1 Conclusion

To show the synergy of top-down photolithography and bottom-up self assembly, we have developed a method for mask-less EPD method patterning devices, thin flexible transparent conductive electrodes for diverse applications, and programmable DNA photolithography using a thymine dimer, which has selectively blocked the information of thymines at a 254 nm sensitive wavelength.

More specifically, we have achieved these:

(1) We have developed a novel method for the macroscale, maskless patterning of biomaterials and nanomaterials onto electrode array devices, which can be applied to electrical fields individually. Our devices, based on the electrophoretic deposition method, are integrated with 400 individual electrode sites. The control of the applied voltage and the deposition time of the individual 400 array electrodes can allow for the optimization of material deposition for macro patterning. Nanoparticles are deposited via programmed patterns using our assembly device, and do not require a mask. Furthermore, our device is reusable, coating layers on the electrode array. Finally, we demonstrate that carbon materials such as carbon nanotubes and graphene oxide can be deposited onto the coating layer, and can be removed from the 400-electrode site array through a relatively simple lift-off process.

(2) We demonstrate a simple, reproducible electrophoretic deposition method for uniform carbon nanotube films using a nitrocellulose membrane. This unique method with the nitrocellulose membrane allows us to produce a transparent flexible carbon nanotube network film with mechanical strength. Most importantly, after solvent

treatment, the opaque substrate changed to transparent with conductivity. Thus, we produced flexible transparent films. Another unique aspect is that after solvent treatment, the substrate had mechanical strength, unlike the free stranding nanoparticles. The key to the new process is that nitrocellulose materials hold carbon nanotubes networks from a free stranding status that has mechanically weak binding. This means that no additional process is necessary to enhance the binding property. In addition, the endurance of the transparent conductive electrodes was tested 4700 times by bending and 180^{o} folding. Finally, we have been able to demonstrate patterned carbon nanotubes using patterned electrodes.

(3) We demonstrate the diverse transmittance nitrocellulose membrane depending on surface morphology through solvent treatment. Most importantly, after solvent treatment, the porous nitrocellulose membrane changed to a high transparent uniform substrate without pores through melting and reconstruction. This unique solvent treatment method with the nitrocellulose membrane can be easily combined with several methods: Electrophoretic deposition, laser printing, shadow masked metal sputtering deposition, spraying carbon nanotubes, and dying for optical filters. The silver nanowire–fabricated nitrocellulose by electrophoretic deposition has been successfully implanted into newspaper without losing conductivity (17 Ω/sq). Furthermore, this flexible nitrocellulose film can be implanted into diverse surfaces such as textiles, plastic key chains and glass surfaces.

(4) We demonstrate a submicron pattern in DNA and a uniform DNA macro-scale pattern using the phenomenon of the dimerization of thymine by photolithography, a common semiconductor manufacture technique. This technology

allows a single-level pattern or a double-level pattern with a target sequence and binding streptavidin-biotin-DNA. With this technique, combined with the photolithography method, the benefits include that it is a simple binding method, is large-scale, has submicron-size resolution, and can perform multiple binding without a heat control system. We believe that these results show that this technique will influence DNA nanoparticle self-assembly or high-resolution protein studies for DNA microarray sequence chips or DNA computing as future work.

6.2 Future Work

We believe that the EFD-LBL devices, systems, and methods represent a unique synergy of combining the best aspects of "top-down" and "bottom-up" technologies into a viable nano/micro/macrofabrication process. It also represents bio-inspired logic for self-assembly and the hierarchal scaling of nanocomponents into integrated microscopic structures. Some important potential applications for this process include miniaturized chemical and biosensor devices, "micronsize" dispersible chem/bio sensors for environmental and bioagent detection, lab-on-a-chip devices, and *in vivo* diagnostic/drug delivery systems. More applications may be found in photonic and electronic devices (displays, etc.); fuel cells; photovoltaic devices, piezoelectric devices, batteries, hybrid energy collection, storage and conversion devices; such devices are thin, soft and flexible, and include other electronic (CMOS components) and photonic components (displays, etc.). Further uses include novel large-scale hybrid solar/wind (piezoelectric) energy collection, storage and conversion devices for bulk energy production (but can be designed and fabricated into environmentally

pleasing forms), nanostructured materials, and highly heterogeneous smart nanomorphing materials and devices.

A DNA double write system relates to novel DNA, RNA, and other modified nucleic acids where thymidine bases are placed at specific locations in the sequence; as such, it allows DNA to be used as a *double write/double identity* photolithographic material for macro-, micro- and nanolithographic patterning, and for three dimensional nanofabrication. DNA *double write* can extend methods, devices, and systems for carrying out masked photolithography and for carrying out directed beam writing, including digital projection patterning (DPP) systems. Furthermore, DNA *double write* can be make a synergistic effect with electric field–directed hybridization and self-assembly fabrication to produce complex heterogeneous three dimensional layered materials, structures and devices. We believe that possible applications for the DNA constructs, methods, and processes include but are not limited to: Smart nanomorphing materials, batteries; photovoltaics; fuel cells; catalysts and synthetic enzyme structures; nano/micro integrated electronic and photonic devices; porous electrode/electrolyte/integrated sensor hydrogel materials, structures and devices; cell and tissue engineering scaffolds, matrixes, and structures with integrated sensors; micro/nanoarray genotyping, sequencing, proteomic and drug discovery devices; lab-on-a-chip; point of care, hand held, patch, and *in vivo* diagnostic devices.

References

National Research Council: Small Wonders, Endless Fron- tiers: Review of the National Nanotechnology Initiative. National Academy Press, Washington, DC (2002)

National Science and Technology Council: The National Nanotechnology Initiative – Strategic Plan. National Sci- ence and Technology Council, Washington, DC (2004)

Hughes, M.P. (ed.): Nanoelectromechanics in Engineering and Biology. CRC Press, Boca Raton (2003)

Goddard, W.A., Brenner, D.W., Lyashevski, S.E., Lafrate, G.J. (eds.): Handbook of Nanoscience, Engineering and Technology. CRC Press, Boca Raton (2003)

Bashir, R.: Biological mediated assembly of artificial nanostructures and microstructures. In: Goddard, W.A., Brenner, D.W., Lyashevski, S.E., Lafrate, G.J. (eds.) Handbook of Nanoscience, Engineering and Technology, pp. 15- 1–15-31. CRC Press, Boca Raton (2003)

Heller, M.J., Tullis, R.H.: Self-organizing molecular pho- tonic structures based on functionalized synthetic DNA polymers. Nanotechnology 2, 165–171 (1991)

Hartmann,D.M.,Schwartz,D.,Tu,G.,Heller,M.J.,Esener, S.C.: Selective DNA attachment of particles to substrates. J. Mater. Res. 17(2), 473–478 (2002)

Sosnowski, R.G., Tu, E., Butler, W.F., O'Connell, J.P., Heller, M.J.: Rapid determination of single base mismatch in DNA hybrids by direct electric field control. Proc. Nat. Acad. Sci. USA 94, 1119–1123 (1997)

Heller, M.J., Tu, E., Holmsen, A., Sosnowski, R.G., O'Connell, J.P.: Active microelectronic arrays for DNA hybridization analysis. In: Schena, M. (ed.) DNA Microarrays: A Practical Approach, pp. 167–185. Oxford University Press, New York (1999)

Heller, M.J.: DNA microarray technology: devices, systems and applications. Annu. Rev. Biomed. Eng. 4, 129–153 (2002)

Heller, M.J., Tu, E., Martinsons, R., Anderson, R.R., Gurtner, C., Forster, A., Sosnowski, R.: Active microelec- tronic array systems for DNA hybridization, genotyping, pharmacogenomics and Nanofabrication Applications. In: Dekker, M., (eds.) Integrated Microfabricated Devices, Heller and Guttman, New York, pp. 223–270 (2002)

Gilles, P.N., Wu, D.J., Foster, C.B., Dillion, P.J., Channock, S.J.: Single nucleotide polymorphic discrimination by an electronic dot blot assay on semiconductor microchips'. Nat. Biotechnol. 17(4), 365–370 (1999)

Edman, C.F., Swint, R.B., Gurthner, C., Formosa, R.E., Roh, S.D., Lee, K.E.,

Swanson, P.D., Ackley, D.E., Colman, J.J., Heller, M.J.: Electric field directed assembly of an InGaAs LED onto silicon circuitry. IEEE Photonic. Tech. L. 12(9), 1198–1200 (2000)

US # 6,569,382, Methods and apparatus for the electronic homogeneous assembly and fabrication of devices, issued 27 May 2003

Mirkin, C.A., Letsinger, R.L., Mucic, R.C., Storhoff, J.J.: A DNA-based method for rationally assembling nanoparticles into macroscopic materials. Nature 382, 607–609 (1996)

Mardilovich, P., Kornilovitch, P.: Electrochemical fabrica- tion of nanodimensional multilayer films. Nano Lett. 5(10), 1899–1904 (2005)

Hua, F., Shi, J., Lvov, Y., Cui, T.: Patterning of layer-by- layer self-assembled multiple types of nanoparticle thin films by lithographic technique. Nano Lett. 2(11), 1219–1222 (2002)

Dehlinger, D.A., Sullivan, B., Esener, S., Hodko, D., Swanson, P., Heller, M.J.: Automated combinatorial process for nanofabrication of structures using bioderivatized nanoparticles. J. Assoc. Lab Automation 12(5), 267–276 (2007)

Dehlinger, D.A., Sullivan, B.D., Esener, S., Heller, M.J.: Electric field directed assembly of biomolecular derivatized nanoparticles into higher order structures. Small 3(7), 1237–1244 (2007)

Dehlinger, D.A., Sullivan, B., Esener, S., Heller, M.J.: Directed hybridization of DNA nanoparticles into higher order structures. Nano Lett. 8, 4053–4060 (2008)

Hu, L., Kim, H. S., Lee, J.-Y., Peumans, P., Cui Y., ACS nano 2010, 4, 2955.

Tao, A., Kim, F. , Hess, C. , Goldberger, J., He, R., Sun, Y., Xia, Y., Yang, P., *Nano Lett.* 2003, 3 (9), 1229-1233.

Noh, H., Hung, A. M. , Choi, C., Lee, J. H., Kim, J., Jin, S., Cha, J. N., *ACS Nano* 2009, 3 (8), 2376-2382.

Adams, J. J., Duoss, E. B., Malkowski, T. F., Motala, M. J., Ahn, B. Y., Nuzzo, R. G., Bernhard, J. T., Lewis, J. A., *Adv. Mater.* 2010 23 (11), 1335-1340.

Sun, D., Timmermans, M. Y., Tian, Y., Nasibulin, A. G., Kauppinen, E. I., Kishimoto S., Mizutani, T., Ohno, Y., *Nat. Nanotech.* 2011 6 (3), 156-161

Ammam, M., Fransaer, J., *Biosensors and Bioelectronics* 2009, 25 (1), 191-197

Hsiao, A. P., Heller, M. J., *Journal of Biomedicine and Biotechnology* 2012, 2012, 9

Chang, Y., Huang S., Chen, Y., *Small* 2009, 5 (1), 63-66

O'Riordan, A., Delaney, P., Redmond, G., *Nano Lett.* 2004, 5, 761-765

Edman, C. F., Swint, R. B., Gurtner, C. , Formosa, R. E., Roh, S. D., Lee, K. E., Swanson, P. D., Ackley, D. E., Coleman, J. J., Heller, M. J., Photonics Technology Letters, IEEE 2000, 12, 1198.

Lima, M.D., de Andrade, M. J., Bergmann, C. P., Roth, S., *J. Mater. Chem.*, 2008, 18, 776-779

Zhou, Y., Hu, L., Gruner, G., *Appl. Phys. Lett.* 2006, 88 123109

Li, X., Gittleson, F., Carmo, M., Sekol, R. C., Taylor, A. D., *ACS Nano* 2012 6 (2), 1347-1356.

Chang, C., Hsu K., Liu Y., *Journal of Polymer Science Part B: Polymer Physics* 2012 50 (16), 1151-1155

Hsu, C. W., Zhen, B., Qiu, W., Shapira, O., DeLacy, B. G., Joannopoulos, J. D., Soljacic, M., *Nat. Comms.* 2014, 5, 3152

Nogi, M., Iwamoto, S., Nakagaito, A. N., Yano, H., *Adv. Mater.* 2009, 21 (16), 1595-1598

Okahisa, Y., Yoshida, A., Miyaguchi, S., Yano, H., *Composites Science and Technology* 2009, 69 1958-1961

Huang, J., Zhu, H., Chen, Y., Preston, C., Rohrbach, K., Cumings, J., Hu, L., *ACS Nano* 2013 7 (3), 2106-2113

Fang, Z., Zhu H., Yuan, Y., Ha, D., Zhu, S., Preston, C., Chen, Q., Li, Y., Han, X., Lee, S., Chen, G., Li, T., Munday, J., Huang, J., Hu, L., *Nano Lett.* 2014 14 (2), 765-773.

Koga, H., Nogi, M., Komoda, N., Nge, T. T., Sugahara, T., Suganuma, K., NPG Asia Mater 2014, 6, e93.

Boccaccini, A. R., Cho, J., Roether, J. A., Thomas, B. J. C., Jane Minay, E., Shaffer, M. S. P., Carbon 2006, 44, 3149.

Song, K. W., Costi, R., Bulovic, V., *Adv. Mater.* 2013, 25, 1420-1423

Dehlinger, D. A., Sullivan, B. D., Esner, S., Heller, M. J., *Small* 2007, 3(7), 1237-1244

Galatsis, K., Wang, K. L., Ozkan, M., Ozkan C. S., Huang, Y., Chang, J. P., Monbouquette, H. G., Chan, Y., Nealey, P., Botros, Y., *Adv. Mater.* 2010, 22 769-778

Tobjork, D., Osterbacka, R., *Adv. Mater.* 2011, 23, 1935.

Davis, T.L. *The Chemistry of 12 Powder and Explosives*, Angriff Press,1972 p. 548.

Towbin, H., Staehelin, T., Gordon, J., *Proc.Nat. Acad. Sci. USA* 1979, 76, 4350.

Kyhseandersen, J., *J. Biochem. Biophys. Methods* 1984, 10, 203.

Kurien, B.T.,Scofield, R.H. *Introduction to Protein Blotting. In Protein blotting and detection: methods and protocols.* Humana Press: New York, NY, 2009; 9-22.

Wray, R. I., Vorst, A. R. V., *Ind. Eng. Chem.*1936, 28, 1268.

Esselen, G. J., *Ind. Eng. Chem.* 1934, 26, 26.

Fang, Z., Zhu, H., Yuan, Y., Ha, D., Zhu, S., Preston, C., Chen, Q., Li, Y., Han, X., Lee, S., Chen, G., Li, T., Munday, J., Huang, J., Hu, L., *Nano Lett.* 2013, 14, 765.

Huang, J., Zhu, H., Chen, Y., Preston, C., Rohrbach, K., Cumings, J., Hu, L., *ACS nano* 2013, 7, 2106.

Shih, M.-H., *Nat. Photon.* 2014, 8, 171.

Nandy, S., Banerjee, A., Fortunato, E., Martins, R., *Reviews in Adv. Sci. and Eng.*

2013, 2, 273.

Cheremisinoff, N. P., *Industrial Solvents Handbook,* CRC Press 2003

http://www.nitrex.in/manufacturing.asp

Llobera, A., Demming, S., Joensson, H. N., Vila-Planas, J., Andersson-Svahn, H.,

Buttgenbach, S., *Lab. Chip* 2010, 10, 1987.

Hofmann, O., Wang, X., Cornwell, A., Beecher, S., Raja, A., Bradley, D. D. C.,

deMello, A. J., deMello, J. C., *Lab. Chip* 2006, 6, 981.

Anuj, R. M., Akshay, K., Chongwu, Z., *Nanotechnology* 2011, 22, 245201.

Kim, H., Ge, J., Kim, J., Choi, S.-e., Lee, H., Lee, H., Park, W., Yin, Y., Kwon, S., *Nat. Photon.* 2009, 3, 534.

Zou, J., Li, C.-Z., Chang, C.-Y., Yip, H.-L., Jen, A. K. Y., *Adv. Mater.* 2014, 26, 3618.

Rathmell, A. R., Wiley, B. J., *Adv. Mater.* 2011, 23, 4798.

Tudorache, M., Bala, C., *Anal. Bioanal. Chem.* 2007, 388, 565.

Lu, Y., Shi, W., Qin, J., Lin, B., *Anal. Chem.* 2009, 82, 329.

Søndergaard, R., Hösel, M., Angmo, D., Larsen-Olsen, T. T., Krebs, F. C., *Mater. Today* 2012, 15, 36.

Kawahara, Y., Hodges, S., Cook, B. S., Zhang, C., Abowd, G. D., "Instant inkjet circuits: lab-based inkjet printing to support rapid prototyping of UbiComp devices", presented at *Proc. of the 2013 ACM int. joint conf. on Pervasive and ubiquitous computing*, 2013.

Lipomi, D. J., Vosgueritchian, M., Tee, B. C. K., Hellstrom, S. L., Lee, J. A., Fox, C. H., Bao, Z., *Nat. Nanotechnol.* 2011, 6, 788.

Luther, J. M., Law, M., Beard, M. C., Song, Q., Reese, M. O., Ellingson, R. J., Nozik, A. J., *Nano Lett.* 2008, 8, 3488.

Han, T.-H., Lee, Y., Choi, M.-R., Woo, S.-H., Bae, S.-H., Hong, B. H., Ahn, J.-H., Lee, T.-W., *Nat. Photon.* 2012, 6, 105.

Schur, M. O., Hoos, B. G., *Ind. Eng. Chem.,* 1937, 29, 26.

Woodbridge Jr., R. G., *Paper: Devoted to the manufacture, sale and use of pulp and paper* Volume 26, 1920 ,p136-146

Sibley, C. G., Ahlquist, J. E. The Phylogeny of the Hominoid Primates, as Indicated by DNA-DNA Hybridization. *J. Mol. Evol.* 20, 2-15 (1984).

Gilles, P. N., Wu, D. J., Foster, C. B., Dillon, P. J., Chanock, S. J. Single nucleotide polymorphic discrimination by an electronic dot blot assay on semiconductor microchips. *Nature Biotechnol.* 17, 365-370 (1999).

Sullivan, B. D., Dehlinger, D. A., Zlatanovic, S., Esener, S. A., Heller, M. J. Low-Frequency Electrophoretic Actuation of Nanoscale Optoentropic Transduction

Mechanisms. *Nano Lett.* 7, 950-955 (2007).

Mirkin, C. A., Letsinger, R. L., Mucic, R. C., Storhoff, J. J. A DNA-based method for rationally assembling nanoparticles into macroscopic materials. *Nature* 382, 607-609 (1996).

Noh, H., Hung, A. M., Cha, J. N. Surface-Driven DNA Assembly of Binary Cubic 3D Nanocrystal Superlattices. *Small* 7, 3021-3025 (2011).

Gartner, Z. J., Bertozzi, C. R. Programmed assembly of 3-dimensional microtissues with defined cellular connectivity. *Proc. Natl. Acad. Sci. USA* 106, 4606-4610 (2009).

Zhang, G., Tanii, T., Funatsu, T., Ohdomari, I. Patterning of DNA nanostructures on silicon surface by electron beam lithography of self-assembled monolayer. *Chem. Commun.*, 786-787 (2004).

Barbee, K. D., Chandrangsu, M., Huang, X. Fabrication of DNA Polymer Brush Arrays by Destructive Micropatterning and Rolling-Circle Amplification. *Macromol. Biosci.* 11, 607-617 (2011).

Liu, M., Amro, N. A., Chow, C. S., Liu, G.-y. Production of Nanostructures of DNA on Surfaces. *Nano Lett.* 2, 863-867 (2002).

Demers, L. M., Park, S.-J., Taton, T. A., Li, Z., Mirkin, C. A. Orthogonal Assembly of Nanoparticle Building Blocks on Dip-Pen Nanolithographically Generated Templates of DNA. *Angew. Chem. Int. Edn* 40, 3071-3073 (2001).

Heller, M. J., Cable, J. M. & Esener, S. C. Methods for electronic assembly and fabrication of devices, US Patent 6652808 (2003)

Hartmann, D. M., Heller, M., Esener, S. C., Schwartz, D. & Tu, G. Selective DNA attachment of micro- and nanoscale particles to substrates. *J. Mater. Res.* 17, 473-478 (2002).

Cimino, G. D., Shi, Y. B., Hearst, J. E. Wavelength dependence for the photoreversal of a psoralen-DNA crosslink. *Biochemistry* 25, 3013-3020 (1986).

Kaur, G., Johnston, P. & Saito, K. Photo-reversible dimerisation reactions and their applications in polymeric systems. *Polym. Chem.* 5, 2171-2186 (2014).

Heller M. J. Method for increasing the sensitivity of nucleic acid hybridization assays. US Patents 4824776 (1989)

Green C., Tibbetts C. Reassociation rate limited displacement of DNA strands by

branch migration. *Nucleic Acids Res*. 9(8) 1905–1918 (1981)

Iwai, H. Roadmap for 22nm and beyond. *Microelectron. Eng.* 86, 1520-1528 (2009).

Matsunaga, T., Hieda, K., Nikaido, O. Wavelength dependent formation of thymine dimers and (6-4)photoproducts in DNA by monochromatic ultraviolet light ranging from 150 to 365 nm. *Photochem. Photobiol.* 54, 403-410 (1991).

Helleday, T., Petermann, E., Lundin, C., Hodgson, B., Sharma, R. A. DNA repair pathways as targets for cancer therapy. *Nat. Rev. Cancer* 8, 193-204, (2008).

Pinheiro, A. V., Han, D., Shih, W. M., Yan H. Challenges and opportunities for structural DNA nanotechnology. *Nature Nanotech.* 6, 763-772 (2011).

Douglas, S. M., Bachelet, I., Church, G. M. A Logic-Gated Nanorobot for Targeted Transport of Molecular Payloads. *Science* 335, 831-834 (2012).

Qian, L., Winfree, E., Bruck, J. Neural network computation with DNA strand displacement cascades. *Nature* 475, 368-372 (2011).

Qian, L., Winfree, E. Scaling Up Digital Circuit Computation with DNA Strand Displacement Cascades. *Science* 332, 1196-1201 (2011).

Zhang, D. Y., Seelig, G. Dynamic DNA nanotechnology using strand-displacement reactions. *Nature Chem.* 3, 103-113 (2011).

Niu, J., Hili, R., Liu, D. R. Enzyme-free translation of DNA into sequence-defined synthetic polymers structurally unrelated to nucleic acids. *Nature Chem.* 5, 282-292 (2013).

Lin, BJ. Deep uv lithography. *J.Vac. Sci. and Technol.* 12, 1317-1320 (1975).

International Technology Roadmap for Semiconductors, 2013 edition (http://www.itrs.net/Links/2013ITRS/Home2013.htm).

www.cymer.com

Mottaghi, M. D., Dwyer, C. Thousand-Fold Increase in Optical Storage Density by Polychromatic Address Multiplexing on Self-Assembled DNA Nanostructures. *Adv. Mater.* 25, 3593-3598 (2013).

Cheng J, Sheldon EL, Wu L, Uribe A, Gerrue LO, Carrino J, Heller MJ and O'Connell JP, Preparation and Hybridization Analysis of DNA/RNA from E. coli on Microfabricated Bioelectronic Chips, Nature *Biotechnol.*16, 541-546, (1998)

Venkataraman, S., Dirks, R. M., Rothemund, P. W. K., Winfree, E., Pierce, N. A. An autonomous polymerization motor powered by DNA hybridization. *Nature Nanotech.* 2, 490-494 (2007).

Tian, Y., He, Y., Chen, Y., Yin, P., Mao, C. A DNAzyme That Walks Processively and Autonomously along a One-Dimensional Track. *Angew. Chem. Int. Edn* 44, 4355-4358 (2005).